Authors' submitted manuscript (preprint)
Article published in Journal of Journal of Building Engineering, Vol. 66, 2023.
The final published version available at https://doi.org/10.1016/j.jobe.2023.105941

Potential utilization of regional cashew nutshell ash wastes as a cementitious replacement on the performance and environmental impact of eco-friendly mortar

Manjunath Balasubramanya[1], Claudiane M. Ouellet-Plamondon[2], BB Das[3], Chandrasekhar Bhojaraju[1*]

Graphical abstract

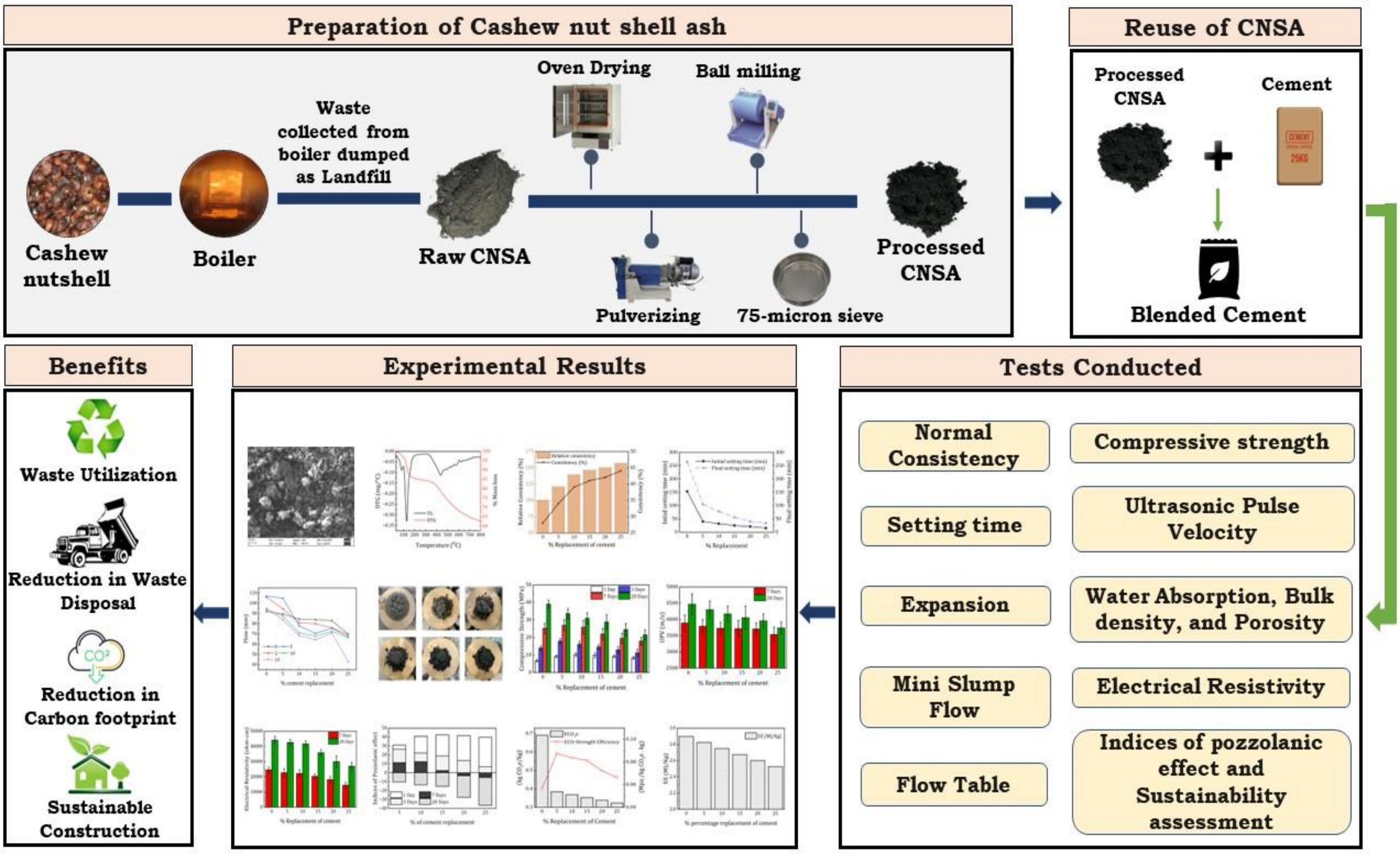

1 Department of Civil Engineering, St. Joseph Engineering College, Vamanjoor, Mangaluru, Karnataka, India. 575028 *(Corresponding author). E-mail address: chandrasekhar.b@sjec.ac.in

2 Department of Construction Engineering, University of Quebec, École de technologie supérieure (ÉTS), 1100 Notre-Dame West, Montréal, QC, H3C 1K3, Canada.

3 Department of Civil Engineering, National Institute of Technology Karnataka, Surathkal, Karnataka 575 025, India

Abstract

Globally, agro-waste ashes are increasing significantly due to the rapid implementation of biomass-based power plants. In the present trend, agro-wastes are disposed of in an unsustainable manner. The recycling of agro-waste has significantly contributed to sustainable goals. In the construction sector, it is possible to dispose of waste more efficiently. However, the efficiency of locally available agro-residual waste in cementitious composites is not well understood. In the present investigation, the practicability of using agro-residual ash obtained from the burning of cashew nut shells on the properties of eco-friendly blended cement paste and mortars is explored. Blended cement mixtures containing cashew nut shell ash (CNSA) were prepared at five replacement levels, 5, 10, 15, 20, and 25%, relative to the weight of the cement. To understand the characteristics of CNSA, microstructure investigations such as X-ray diffraction, thermogravimetric analysis (TGA), scanning electron microscopy, and energy-dispersive spectroscopy analyses were performed. Paste properties of CNSA-based cement are observed through consistency, setting time, mini-slump flow, and expansion tests. For the CNSA-based mortars flow table, compressive strength, ultrasonic pulse velocity (UPV), electrical resistivity (ER), water absorption, Bulk density, and porosity tests were performed to understand its efficiency. The strength indices of mortars were used to quantify the pozzolanic effect of CNSA. With the incorporation of CNSA, water demand increased by 57%, initial and final setting time decreased by 90% and 83%, respectively. Results showed that CNSA-based mortars absorbed more water and had higher porosity, which reduced compressive strength, UPV, and ER values. CNSA blended mortar is more suitable for applications that do not require high compressive strength. Results indicated that the compressive strength, UPV, and ER are within the limit specified. Strength indices indicated that CNSA has a positive and negative pozzolanic effect during early and later ages, respectively. Further, the sustainable assessment showed that the introduction of CNSA in mortar could substantially reduce embodied carbon, embodied energy, and strength efficiency over the control mortar. The inadequate amount of SiO_2, Fe_2O_3, and Al_2O_3 in CNSA makes it an unsuitable pozzolanic material. However, it can be utilized in smaller amounts as a fractional replacement of cement and is found to be promising for specific desired properties of cement as a cost-effective accelerator.

Keywords:

Supplementary cementitious material, Cashew nut shell ash, Blended cement, early age strength, Sustainable assessment

Highlights:

- CNSA improves early-age strength due to its high alkali content and accelerates hydration at an early age.
- CNSA blended mortars can be used for applications that do not require high compressive strength.
- CNSA is a regional waste material that can be used in smaller amounts.
- CNSA is found to be promising for specific characteristics of cement as a cost-effective accelerator.

Abbreviations:

CAGR	Compound annual growth rate	XRD	X-ray diffraction
MMT	Million metric tonnes	SEM	Scanning electron microscopy
SCM	Supplementary cementitious materials	EDS	Energy dispersive spectroscopy
CNSA	Cashew nutshell ash	TGA	Thermogravimetric analysis
CNS	Cashew nutshell	DTG	Derivative Thermogravity
CNSC	Cashew nut shell cake	LOI	Loss on ignition
SCC	Self-compacting concrete	IST	Initial setting time
RAP	Reclaimed asphalt pavement	FST	Final Setting time
SAI	Strength activity index	UPV	Ultrasonic pulse velocity
BBDA	Box–Behnken design approach	ER	Electrical resistivity
OPC	Ordinary Portland Cement	MUV	Multi-Utility vehicle
XRF	X-ray fluorescence	ASTM	American Society for Testing and Materials

1. Introduction

The global cement market is expected to reach USD 488.4 billion by 2027, with a compound annual growth rate (CAGR) of 6.1%. India is the second-largest cement producer in the world [1] and accounts for a 7.8% share of global production. The cement industry will play an important role in building a new India, with cement demands forecast to double by 2030. Cement production in India is envisioned to reach 660 MMT by 2030 at a CAGR of 6.6%. Fig.1 shows the Projected cement demand (MMT) and per capita consumption (kg), 2018 – 2030 of Indian cement. The escalating population and improved industrialization are the main reasons for the significant demand for cement. Population growth has ensued in increased needs for infrastructure and housing. This has surged the demand for cement across the globe for substantiating the facilities in the form of residential, office, healthcare centers, and industrial buildings to support life activities [2]. The construction sector is one of the fastest-growing sectors worldwide. Cement is an essential building material used in construction [3]. Hence, the growing demand from the expanding construction sector is currently influencing the market.

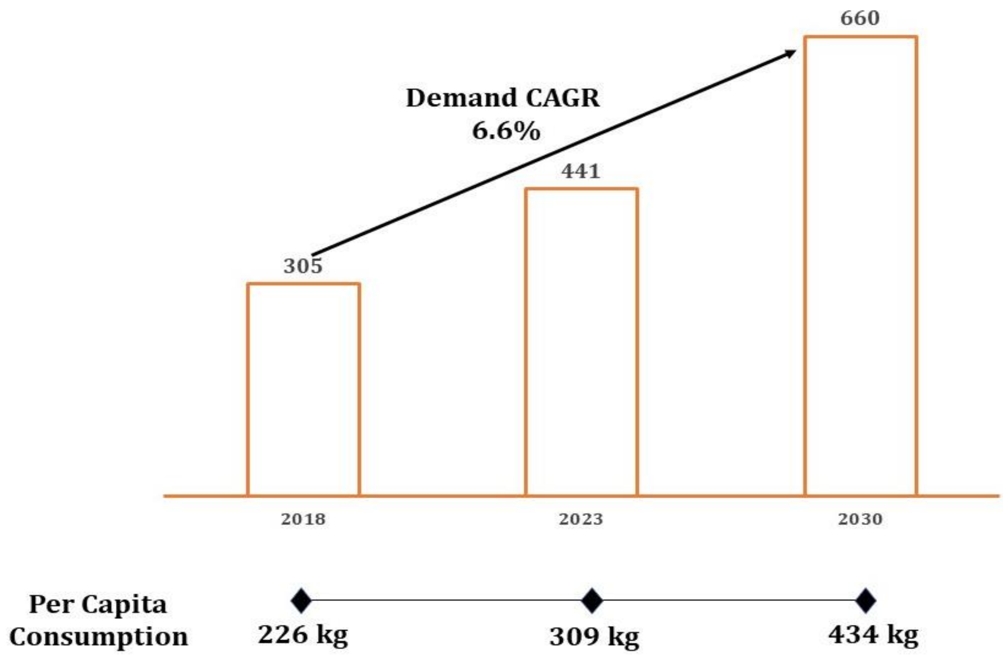

Fig.1: Projected cement demand (MMT) and per capita consumption (kg), 2018 – 2030
(Source: Kanvic Cement Demand Projection Model 2018)[4]

Compared to other industries, pollution from the cement industry is significant that sustainability should be prioritized among issues related to cement production [5]. Due to the energy-intensive processes involved in cement manufacturing, carbon dioxide (CO_2)

constitutes the majority of greenhouse gas emissions [6]. Carbon emissions from the cement industry could increase 27% by 2050 from their current discharge of 5-8% of global CO_2 emissions [7-9]. 39% of energy-related carbon emissions are generated by the building and construction industry [10].

The cement organization is accountable for the over-extraction and consumption of raw material and energy resources, making its manufacturing highly unsustainable [11]. The huge demand for cement as a building material has led to a concern about its substitute with supplementary cementitious materials (SCM). Industrial and agricultural-based remains are the most feasible alternatives for the cement binder [12]. Therefore, the construction industry is motivated to use these remains as construction materials [13]. Researchers have previously investigated the possibility of reusing industrial derivatives as partial alternatives for cement. Fly ash and slag are commonly used industrial residues as SCM [14]. The prolonged obtainability of fly ash is also in doubt, as coal-based electricity development is not a tenable process [15]. It was reported that the slag production is less than 10% of the cement production. However, the accessibility of these residues is reported to be limited [16]. Hence, diversified SCMs need to be interposed against the fast-increasing societal pressure to attain sustainability [17].

The utilization of agricultural waste ashes is a more cost-effective alternative to fly ash and slag since their logistic price is significantly lower. The agricultural residue ashes are locally available to cement plants and ready-mix concrete plants, reducing the transportation of fly ash or slag over long distances [18]. Therefore, the paramount focus of the development and characterization of SCMs has been accorded with by-products from the agro-sector [19]. Agro-based residue ashes as SCMs may proffer economic feasibility, green conservation, and society's endorsement as the three pillars of sustainable development [20].

Several studies have been conducted to analyze the efficacy of diverse agro-industrial residues such as rice husks ashes, bagasse ashes, bamboo leaves ashes, corn cob ashes, banana leaves, palm oil fuel ashes, elephant grass ashes, tea ash, tobacco ash, barley straw, wheat straw, hazelnut, pistachio shell, Rice straw ash [2, 11, 13, 21-31], have shown pozzolanic activity and been used as a fractional substitute in binary blend cement. There have been several studies on using agro-based residue ashes, but there have been limited studies on CNSA. The feasibility of using CNSA as a cement substitute should be assessed.

Cashew nut is a cash crop found in India, Africa, Brazil, Vietnam, and Central America, Portuguese explorers introduced the cashew tree (Anacardium occidentale) to India nearly five centuries ago [32]. Cashew is one of the major horticultural crops, and India is the second-largest producer, processor, and exporter of cashews, with more than 15% of the world's export share. As a marketable commodity, cashew has a crucial role in the liberalized Indian economy. In India, Cashew was cultivated on a total of 1.02 million hectares of land, with a productivity of 706 kg/ha as of 2020. Fig.2 indicates the production of Cashew Nut and CNSA in India. The country's approximate raw cashew by 2050 is estimated to be 4-5 million metric tons or more. India is one of the world's topmost cashew nut-producing countries, and it has 3650 cashew processing industries spread across the states [33]. Some of India's top cashew nut-producing states are Maharashtra, Andhra Pradesh, Orissa, Karnataka, Kerala, and Tamil Nadu.

The cashew shell waste (CNS) generated in small-scale cashew processing industries was found to be 67.5% of total weight of cashew seed [34]. The CNS is dispatched to an oil extraction factory to remove the oil that remains in the cashew nut shell [35]. The product obtained from the oil extrication of CNS is cashew nut shell cake (CNSC). The CNSC is transformed into CNSA by two methods, open burning and burning in a muffle furnace at high temperatures. In addition, CNSA can also be obtained from the boilers of biomass power plants. CNSA obtained from the boilers are usually disposed of in open fields, causing landfill issues. CNSA can be used as a fertilizer for some plants due to its high concentration of nutrients as well as a soil stabilizer [36]. Also, the impact of these ashes on the cement replacement is still at a very early stage of research. Considering this, the study is carried out to utilize CNSA as an SCM in mortar.

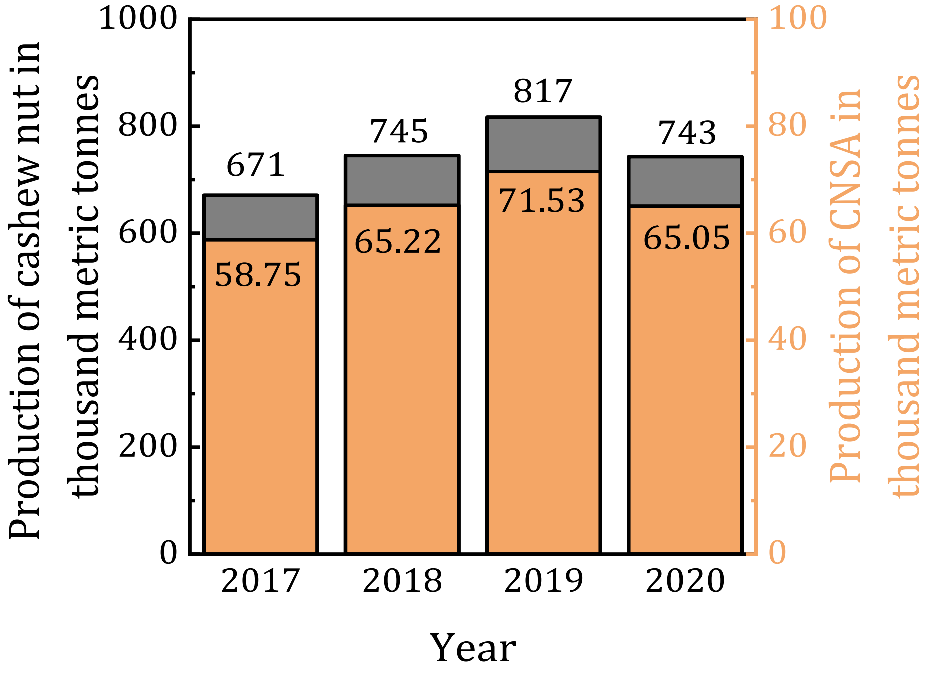

Fig.2: Production of Cashew Nut and CNSA (thousand metric tons) in India, 2017 - 2020

Until now, there are few research on using CNSA as a building material in civil engineering practice. Solomon et al. [37] evaluated the performance of CNSA as a potential binder in concrete production. Results inferred that the workability is increased with a surge in the percentage of CNSA. Adithya Tantri et al. [38] produced a sustainable self-compacting concrete (SCC) incorporating CNSA as a cementitious material and reclaimed asphalt pavement (RAP) as coarse aggregate. Results revealed that CNSA up to 15% was found to be optimum for Ordinary Portland cement (OPC), and the results confirmed that CNSA could be a potential SCM in the future. Utilizing reactivity index concepts and mix proportions, Solomon Oyebisi et al. [39] predicted the splitting tensile strength of concrete embracing Anacardium occidentale nutshell ash. Jugal Kishore Mendu et al. [40] prepared the concrete incorporating CNSA as a partial substitution to cement at 5%, 10%, 15%, and 20% of CNSA to study fresh concrete and hardened properties. He concluded that CNSA has a good pozzolan as the strength activity index (SAI) is more significant than 75%. As indicated in previous findings, mechanical properties of the concrete increased upto15% replacement level [37-39], and the formation of CSH gel is more prominent. CNSA exhibited higher resistance against sulphate than OPC [37, 41]. Additionally, the material showed stronger compressive, splitting, impact, tensile, and bending characteristics than conventional concrete. Solomon Oyebisi et al. [42] used the Box –Behnken design approach (BBDA) to investigate the concrete workability and strength, incorporating binding, water/binder ratio, binder/aggregate ratio, and curing mechanisms. Results indicated that the feasibility of using less water to optimize concrete strength is achievable by blending OPC with CNSA.

Based on the literature, a knowledge gap exists in exploring the potential use of CNSA as a cement alternative, specifically for normal strength preparation in a mortar. This research aims to develop sustainable mortar using CNSA obtained by combusting cashew shells in a boiler at a processing plant with partial substitution of cement. The present research is a portion of more comprehensive research examining the potential use of regionally accessible remains as a binder. The cement and concrete industries may be able to recycle some of these biomass ashes into supplementary products if they possess sufficient SCM potential. It also ensures that these wastes can be disposed of without enduring heavy costs and wide spaces for land disposal.

To explore the use of CNSA as a viable alternative SCM, X-ray fluorescence (XRF), X-ray diffraction (XRD), scanning electron microscopy (SEM), and energy-dispersive spectroscopy (EDS) was performed. The objectives of this study were to

i) Carry out an in-depth analytical characterization-based performance evaluation of CNSA.

ii) Investigate the effect of CNSA on the characteristics of cement paste.

iii) Examine the mechanical characteristics and durability properties of the CNSA based mortars.

iv) Evaluate the sustainability and cost performance of CNSA on the various mixes.

An extensive experimental program has been carried out to answer these objectives. To investigate the characterization of CNSA different microstructural analysis is performed, including a) XRD, b) TGA, c) SEM – EDS. For Fresh properties of the CNSA based paste, various tests like a) Consistency b) Setting time c) Mini-Slump flow d) Expansion tests are considered. Moreover, the present study considers various mechanical and durability tests on CNSA based mortar to address the third objective. The last objective was determined using embodied carbon, embodied energy and eco-strength efficiency.

2. Experimental Information

2.1 Materials

2.1.1 Cement, Fine aggregates, and water

Commercially available OPC (53 grade) conforming to Type – I ASTM C 150 was the primary binder. The chemical compositions of OPC are shown in Table 1. The normal consistency is 28%, the specific gravity is 3.14, 153 min initial setting time (IST), 265 min (FST), and the specific surface area of OPC were 316 m^2/kg, respectively. All the values were within the expected range, conforming to IS 12269 for 53-grade cement. Natural river sand was used as a fine aggregate. The aggregates were washed to remove fine particles, sundried, sieved, and then graded. There is a risk of deleterious reactions with increasing aggregate reactivity. Aggregate reactivity can be prevented by selecting "non-deleteriously" aggregates [43]. The aggregates used in this study are crystalline quartz aggregates and these aggregates are less susceptible to the reactivity [44, 45]. The aggregates passing through a 2.36 mm sieve and retained on a 300μm sieve with a maximum particle size of 2.36 mm were used in this study. The specific gravity of fine aggregate is 2.62, with a fineness modulus of 2.60. The palatable water was used to mix and cure concrete with pH = 7.

2.1.2 Cashew nut shell ash

For this study, CNSA was collected from Kalbhavi cashews, Mangalore, Karnataka, India. CNSA is obtained after the cashew nut shell wastes were dried and burned in a cogeneration boiler. After the burning process, the CNSA is then aggregated, and dumped at the nearest disposal site, thus creating landfill problems. The step-by-step method for developing CNSA is shown in Fig. 5. CNSA collected from a disposal site was dried at 105–110^{0}C for 24 hours to remove any moisture content and cooled at ambient temperature. Subsequently, after the cooling, to increase the reactivity of the particles, the CNSA was pulverized and followed by grinding in a laboratory ball mill for one hour. It has been reported that biomass ash sifted through a 75µm sieve can be used to replace cement in [2, 46]. In this study, CNSA was prepared in a similar manner. Fig.3 delineates the raw and processed CNSA, respectively. The CNSA exhibited lower specific gravity than OPC (i.e., 1.92). The particle size distribution of CNSA is represented in Fig.6. A laser diffraction particle size analyzer was used to measure particle size distribution of CNSA. The particle size distribution in Fig.6 suggests that the D10 (i.e., the diameter of the particles at 10% passing), D50 and D90 values of CNSA are 5.37µm, 18.68µm and 40.02µm respectively which meant 10%, 50%, and 90% of the sample is smaller than 5.37µm, 18.68µm and 40.02µm. The mean diameter of CNSA is 21.16µm. The results from the SEM confirms that CNSA consists of small to bigger particle sizes. The specific surface area of CNSA is 355 m^2/kg by Blaine's air permeability apparatus as per IS 4031 (Part 2)-1995. The oxide composition of OPC and CNSA was determined using XRF. The results are presented in Table 1. By comparing samples' weights before and after ignition for 60 minutes at 750^0 C, the loss on ignition (LOI) values of the CNSA were determined as seen in Fig.4.

(a) (b)

Fig. 3: (a) Raw (b) processed CNSA

Fig. 4: Sample before and after LOI (calcined at 750^{0}C)

Fig.5: step – by – step procedure for the generation of CNSA

Table 1: Physical and chemical properties of binders

Material	Parameters	Chemical composition	OPC	OPC requirements as per ASTM C 150	CNSA
Physical properties	Specific Gravity		3.14	3.15	1.92
	Specific surface area (m^2/kg)		316	225	355
	Pass through a 75µm sieve (%)		100	-	100
	Pass through a 53µm sieve (%)		90	-	72
	Moisture content (%)		-	-	5.88
Chemical properties		Silicon dioxide, SiO_2	18.90	18 - 24	5.73
		Aluminium oxide, Al_2O_3	4.88	2.6 – 8.0	1.50
		Iron oxide, Fe_2O_3	5.28	1.5 – 7.0	3.24
		Calcium oxide, CaO	62.70	61 – 69	11.20
		Magnesium oxide, MgO	1.01	0.5 – 4.0	16.30
		Sulphur trioxide, SO_3	1.16	0.2 – 4.0	0.20
		Sodium oxide, Na_2O	0.38	-	3.02
		Potassium oxide, K_2O	0.50	0.2 – 1.0	42.60
		Phosphorous Pentoxide, P_2O_5	0.23	-	9.73
		LOI	1.25	5.0 max	4.50

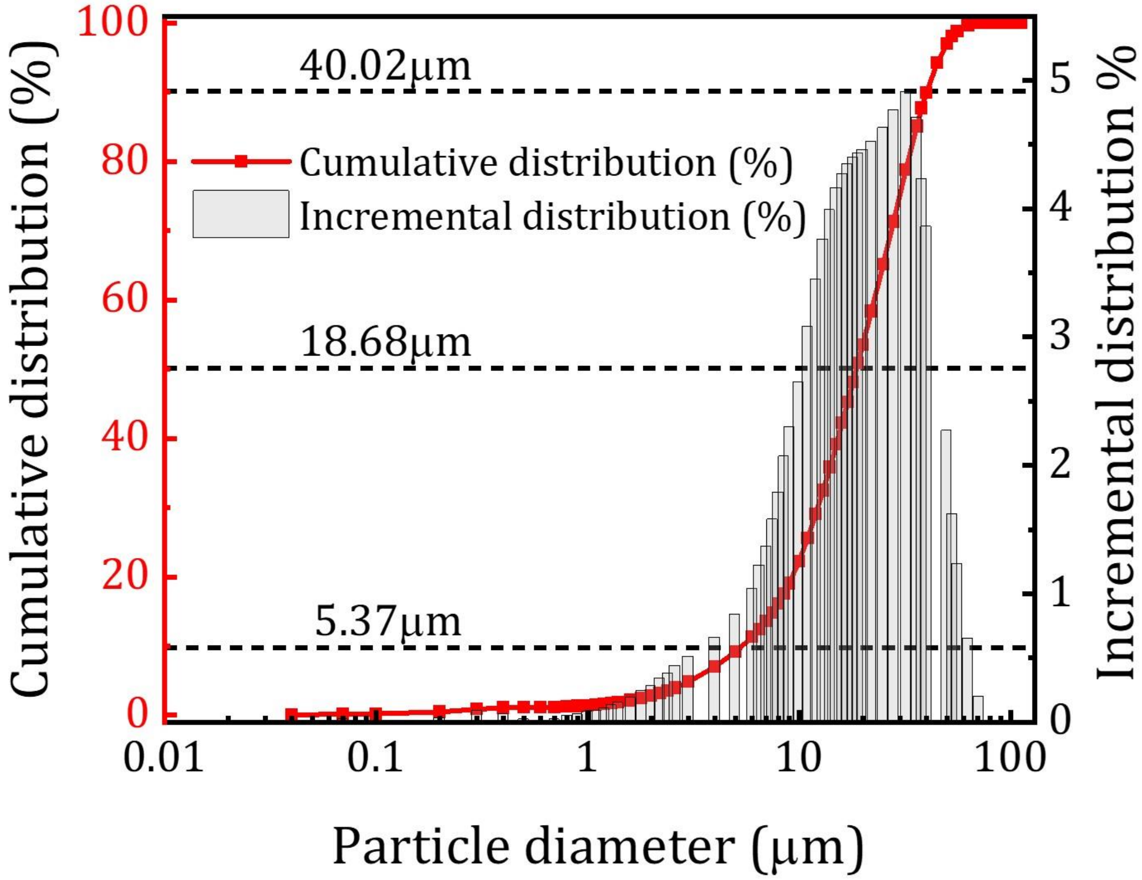

Fig. 6: Particle size distribution of CNSA

2.2 Mortar mix proportions and specimen fabrication

CNSA-based blended cement pastes and mortars were prepared with a CNSA dosage of 5, 10, 15, 20, and 25% relative to the weight of cement using a w/cm ratio and sand/cm ratio of 0.5 and 2.75, respectively. According to [41, 42] studies, specimens were cast with a water-cement ratio of 0.5. The mix proportions for control and CNSA-based blended cement pastes and mortars are presented in Table 2 and 3, respectively.

A study was conducted to evaluate the consistency, setting time, soundness, and acid attack of two types of pastes: i) control cement paste (0CNSA) and ii) CNSA-based blended cement paste. Cement paste was prepared using IKA RW 20 digital high-speed stirrer with a maximum speed of 2000 rpm, as shown in Fig. 8.

All cement mortar mixes were prepared using a standard Digi mortar mixer shown in Fig. 8 according to IS 2250 - 1981 guidelines. In the beginning, all the materials (cement, sand, CNSA, and water) are mixed manually. In order to attain homogeneity, the dry materials are mixed at low speed for one minute and 30 sec at high speed, and the mortar is left to rest for 90 sec to clean the sides of the bowl. The material is further mixed for one minute at high speed. The IS 4031 (Part 7) -1988 was comprehended to determine the workability of mortar through the flow table. A flow diameter of 152 mm was measured for the control mixture. Each mortar mix was kept more than or equal to the flow value of 110 ± 5 mm

Table 2: Mix Proportions of CNSA-based blended cement paste

Mix ID	OPC (g)	Water (g)	CNSA (g)
0 CNSA	400	200	0
5 CNSA	380		20
10 CNSA	360		40
15 CNSA	340		60
20 CNSA	320		80
25 CNSA	300		100

Table 3: Mix Proportions of CNSA-based blended cement mortar

Mix ID	OPC (g)	Sand (g)	Water (g)	CNSA (g)
0 CNSA	450	1238	225	0
5 CNSA	427.5			22.5
10 CNSA	405			45
15 CNSA	382.5			67.5
20 CNSA	360			90
25 CNSA	337.5			112.5

2.3 Testing Methods

2.3.1 Characterization of CNSA

XRF: The chemical characteristics of CNSA were studied using the XRF technique. Bruker model S8 Tiger and S4 Pioneer sequential wavelength-dispersive X-ray spectrometers and sample preparation units were used with a 4 kW Rh X-ray tube. Also, SPECTRA plus software for the qualitative and quantitative determination of elements.

XRD: XRD technique was used to study the mineralogical characteristics of the CNSA sample. A 3rd generation Empyrean, Malvern PANalytical with 2θ linearity equal or better than ± 0.01° and angular resolution of 0.026°, scanning from 10^0 to 80^0 (2θ), with 10^0 intervals.

DTA/TGA: TGA quantifies changes in physical and chemical properties of materials with accelerating temperature at a constant rate. TGA defines the properties of materials that exhibit decomposition, oxidation, or loss of volatiles that affect their mass. In this study, TGA 4000, PerkinElmer of maximum temperature 800^0C at a heating rate of 10^0 C/min was used to study the properties of CNSA.

SEM: The scanning electron microscopy (SEM) technique was used to envision the microstructure and morphology of CNSA. SEM was studied using Carl Zeiss, GEMINI 300.

2.3.2 Tests on Blended pastes and mortars

Vicat apparatus was used to assess the consistency of the control and CNSA-based cement paste samples according to ASTM C187 -16 [47]. The amount of water required must be determined to obtain adequate consistency of cement paste [13].

IST is the period between cement contact with water and penetration measurement. After the cement is initially in contact with water, the FST is measured when the needle leaves no full circular impression on the paste surface. Vicat apparatus was used to evaluate the setting time of the control and CNSA-based cement paste samples according to ASTM C 191-08 [48].

An expansion or soundness indicates a hardened binder paste's ability to resist expansion when excessive magnesia or free lime is present. The expansion of the control and blended specimens are according to BS EN 196-3 [49].

A miniature design of the Abrams test was considered for the mini-slump tests that showed the same characteristic of the cone described in ASTM C1437 [50]. Freshly prepared pastes were filled in a reduced version of the slump cone with a top diameter of 19 mm, bottom diameter of 38 mm, and height of 57 mm, which was placed on a grid-marked plate. In the first stage, dry materials are mixed at 200 rpm at 60 sec, water is added to 300 g of cement, and then mixed for 60 sec at 500 rpm. The cement paste is left to rest for 90 sec in the next stage. In the last step, the paste is continuously mixed for 90 sec at 2000 rpm. After mixing, the fresh pastes were tested for flow using a mini-slump cone. After lifting the filled cone, the cement paste’s flow to a stable state, and the increase in the diameter of the cone is measured in perpendicular directions to determine its diameter. The photo is taken from the top of the arrangement. Fig. 7 illustrates the procedure used to carry out the mini-slump flow test.

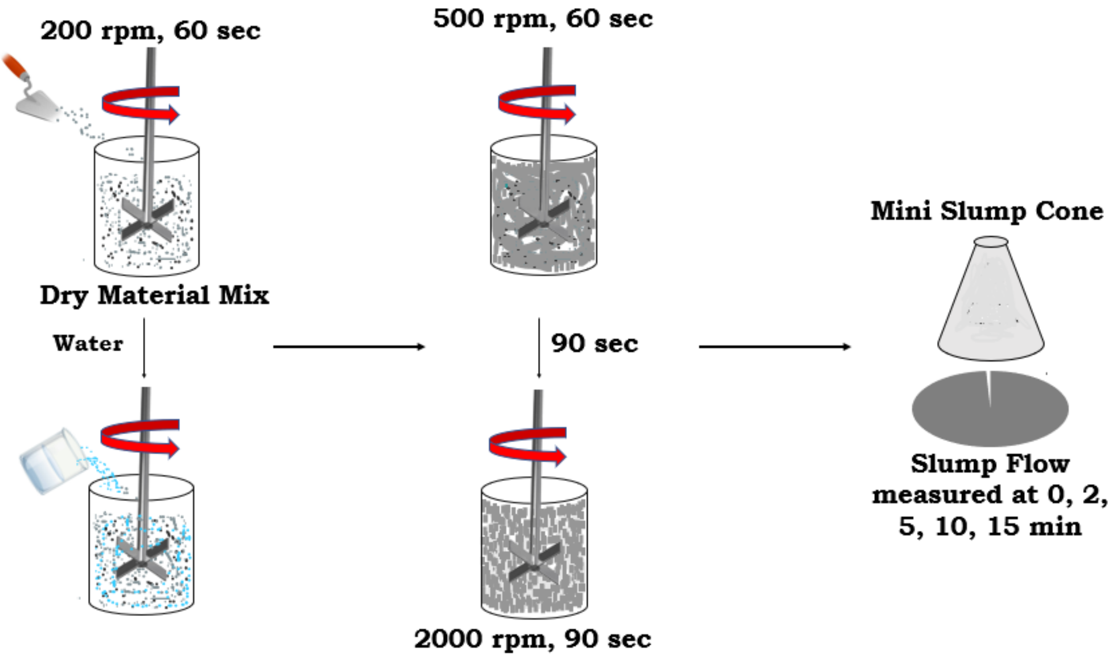

Fig. 7: Procedure used to determine mini-slump

(a) (b) (c)

Fig. 8: Apparatus (a) high-speed stirrer (b) Digi mortar mixer (c) flow table

After 28 days of water curing, the compressive strength of CNSA-based mortar was determined using 50mm as recommended by ASTM C109 [51]. Based on ASTM C642–13 [52], bulk density, water absorption, and porosity measurements were performed on mortar specimens. Eq. (1,2,3) was used to calculate absorption, density, and porosity for each mixed sample. The values reported are the averages obtained from testing three mortar samples per mix proportion.

Absorption after immersion, % = $[(W_2 – W_1) / W_1] \times 100$ (1)

Bulk Density, dry = $[(W_1/ (W_3 – W_4)] \times 100$ (2)

Porosity = $[(W_3 – W_1) / (W_3 – W_4)] \times 100$ (3)

W_1 = weight of the specimens dried in an oven at 105^0C for 24h

W_2 = weight was measured immediately to obtain the weight of the sample in water mass of surface-dry sample in the air after immersion

W_3 = surface of the cube specimens was wiped with a clean towel and reweighed for the saturated surface dry weight in the air after immersion and boiling.

W_4 = Apparent mass of sample in water after immersion and boiling

The UPV of the cured cubic mortar samples was determined using the PUNDIT portable ultrasonic device, following ASTM C597 [53]. During this test, the pulse velocity traveling through the cement composite medium is measured to detect cracks and voids.

Cubic mortar samples were tested for ER after 7 and 28 days of curing. To measure resistivity, two electrodes were connected to two sides of the samples [13, 54], and an electrical resistance measurement instrument was used, as shown in Fig. 9. Based on the formula = RA/L, the resistivity values ρ were determined. Where ρ is the resistivity (Ω-cm), R is the resistance (Ω), A is the sample area (cm^2), and L is specimen length (cm). An Analytical method is used to evaluate the pozzolanic effect of CNSA as a cement substitute in mortar and was conducted in accordance with the foregoing studies by [2, 55]. Table 4 indicates the summary of the tests conducted in this study. In addition, SEM was performed on the chosen mixes to determine the influence of CNSA on the microstructure of mortar.

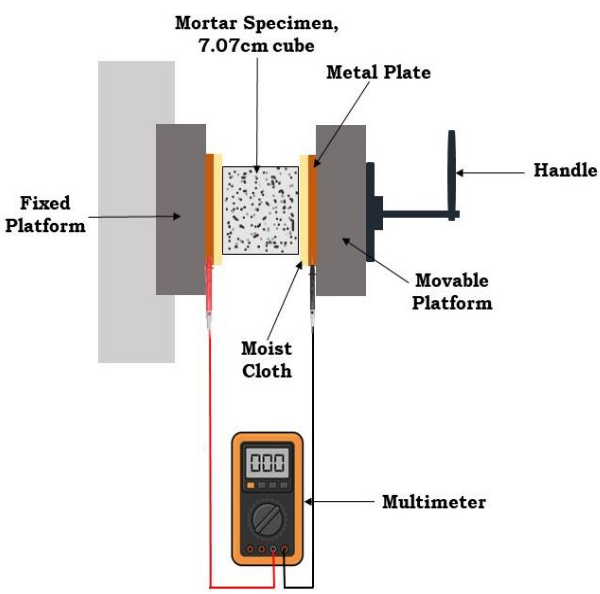

Fig. 9: Testing Method for determining electrical resistivity of mortar

Table 4: Summary of the tests methods conducted in this study

Sl. No	Tests performed	Specimen	Size of the Specimen	Curing time	Number of samples per mix	Standards used in this study
Paste						
1	Consistency		-	-	-	ASTM C187 -16
2	Setting time		-	-	-	ASTM C191 -08
3	Expansion	OPC and Blended Pastes	-	-	2	BS EN 196-3
4	Mini Slump		Top dia = 19 mm, Bottom dia = 38 mm, and height = 58 mm	-	-	ASTM C1437
Mortar						
6	Flow table		-	-	-	ASTM C1437
7	Compressive Strength		50 x 50 x 50 mm	1, 3, 7, 28 days	12	ASTM C109
8	Ultrasonic pulse velocity	OPC and Blended Mortar		7, 28 days	6	ASTM C597
9	Water absorption, Bulk density, Porosity		70.6 x 70.6 x 70.6 mm	28 days	6	ASTM C642–13
10	Electrical resistivity			7, 28 days	3	[54]

3. Results and Discussion

3.1 Characterization on CNSA

The chemical composition of the CNSA is presented in Table 1. The CNSA has a high K_2O content, which is in accession with the results reported by [56]. The presence of more than 30% K_2O can cause the fusion of large and dense particles during oxidization [57] which is justified by the SEM image of CNSA. More energy is required to grind these large dense particles to get the desired fineness [24]. Studies showed that the mineral composition of cashew nuts has the highest concentration of potassium (K), followed by magnesium (Mg), Calcium (Ca), phosphorous (P), and sodium (Na) [58-60]. The high K contents of the CNSA could be caused due to the occurrence of more clayey soils under the cashew plantation [61]. Such High alkali (K and Na) levels negatively affect workability, setting, and strength [62]. Table 1 presents the concentration of SiO_2 and Al_2O_3 for the CNSA, which are substantially lesser than the expressed in other research [37, 38, 40]. SCMs with high calcium aluminosilicate concentrations usually exhibit pozzolanic activity. Therefore, the low concentration of SiO_2, Al_2O_3, Fe_2O_3, and CaO in the CNSA will likely result in a low pozzolanic activity. The morphology of CNSA is examined by SEM at various magnifications as shown in Fig. 10, CNSA particles display some aggregation, and are comprised of angular, large, and medium-sized particles than OPC. The EDS analyzes of the CNSA particles are presented in Fig.11. Fig.12 (a) shows the mineral composition of CNSA. The minerals were identified as Calcium silicate ($CaSiO_4$), Arcanite (K_2SO_4), Periclase (MgO), Quartz (SiO_2), Potassium ferrite (K_2FeO_4), Sodium phosphate (Na_3PO_4), Sylvite (KCl), and Harmunite ($CaFe_2O_4$). Harmunite structure is highly crystalline, an oxide semiconductor, and a high anisotropy antiferromagnet [63, 64]. Fig.12 (b) shows that potassium, magnesium, calcium, phosphorous, and silicon are the primary oxides identified by XRF.

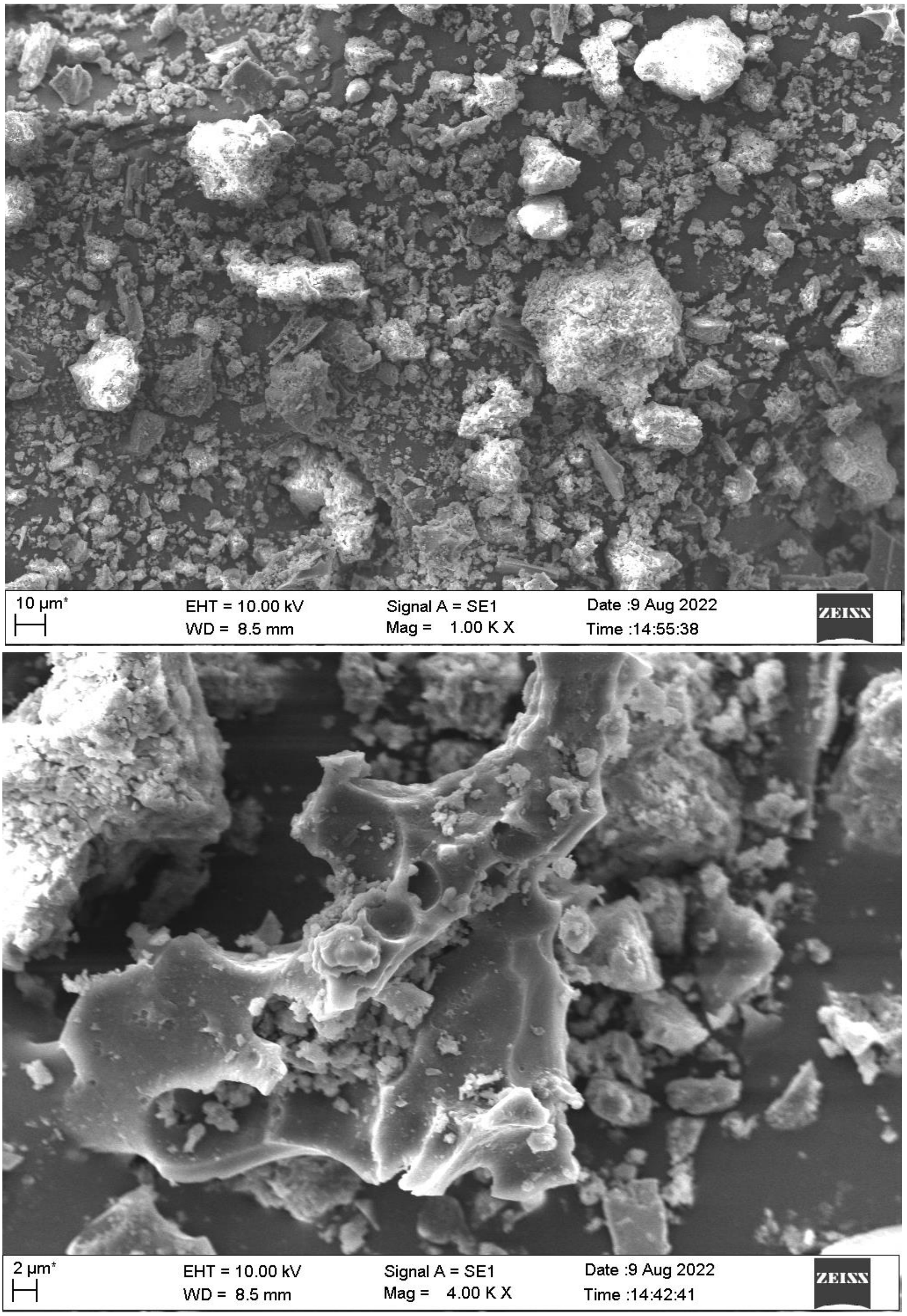

Fig. 10: SEM of CNSA particles at
a) 1.00 K X b) 4.00 K X Magnification

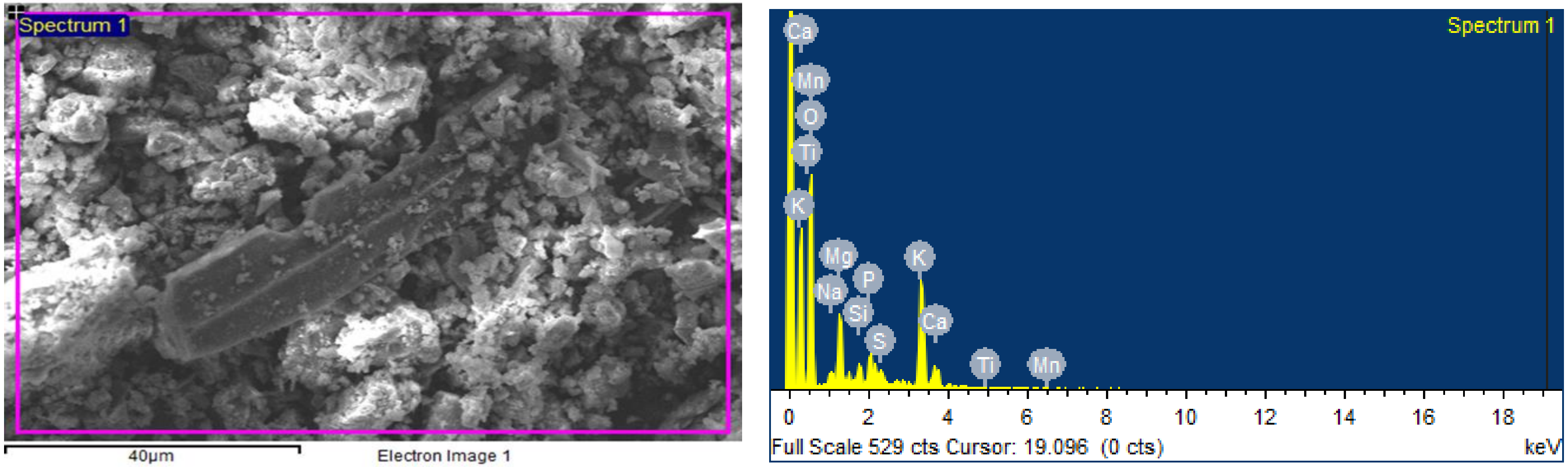

Element	Weight %	Atomic %
Ca K	4.54	2.48
O K	51.30	70.11
Si K	1.87	1.46
K K	27.69	15.49
Na K	1.00	0.95
Mg K	5.85	5.26
P K	2.75	1.94
S K	1.03	0.70
Ti K	0.53	0.24

Fig. 11: EDS analysis of CNSA Particles

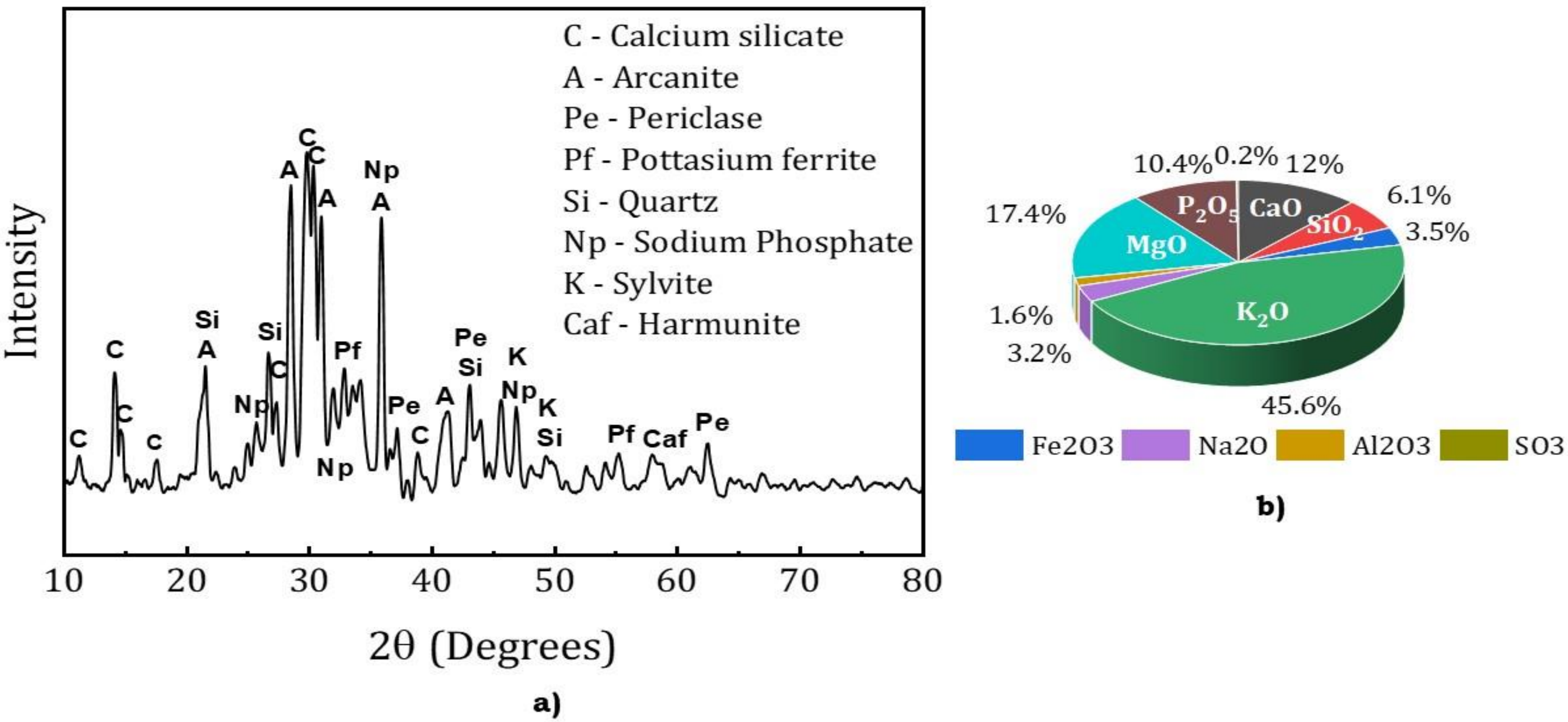

Fig.12: a) XRD pattern of CNSA b) Percentage of oxides in CNSA based on XRF

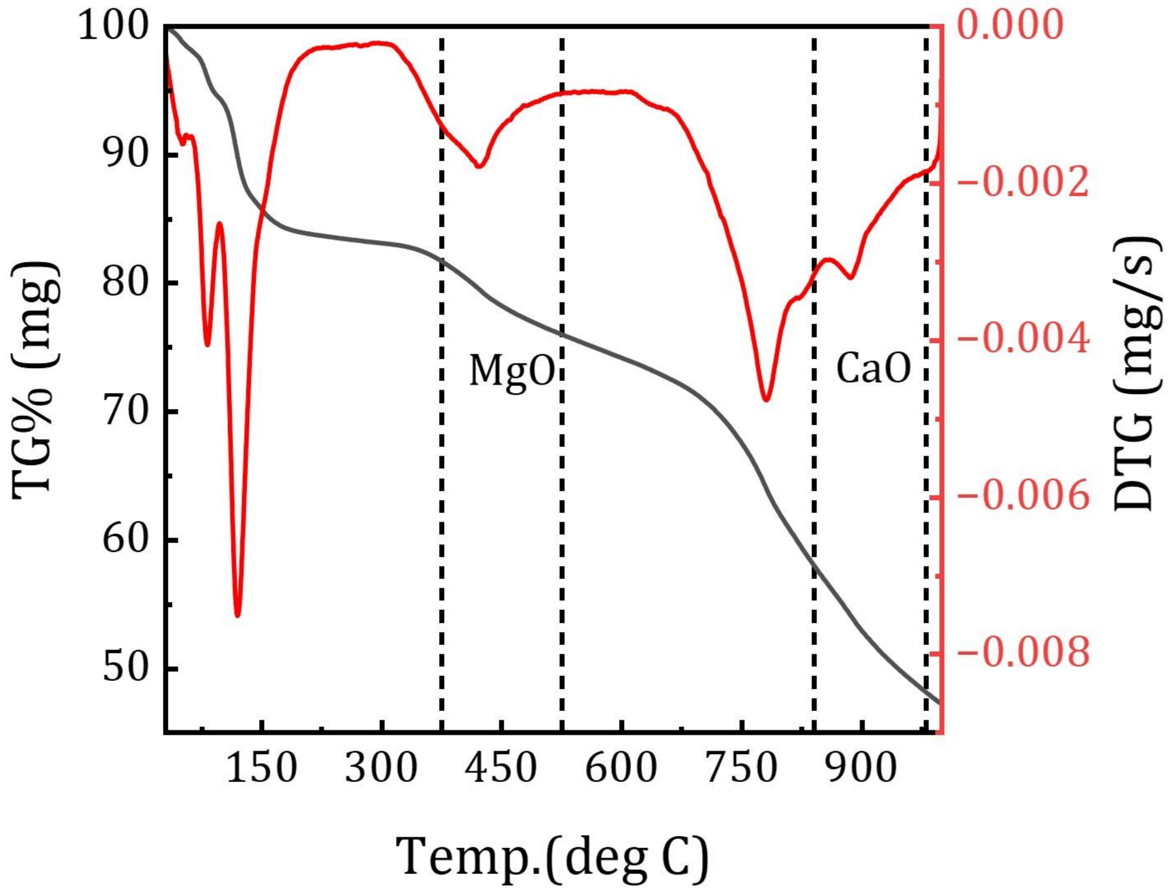

Fig. 13: Thermogravimetric analysis (TGA) of CNSA

Fig. 13 shows the results of the TG – DTG curves of the CNSA. During the first phase, initial moisture is evacuated with a peak temperature of 72^0C. In the second phase, hemicellulose dissipates between 89^0C and 213^0C, with the maximum removal of hemicellulose detected at 112^0C, as indicated by the curve inflection point. In the third phase, the decomposition of cellulose occurred between 307^0C and 513^0C, with a peak occurring at 412^0C. MgO is a hygroscopic material that can absorb moisture from the air. As a result, the MgO temperature observed in TGA might range between 367^0C to 451^0C, resulting in a weight loss of 24% as a result of removing absorbed water and hydroxide groups. The fourth phase of lignin degradation involves endothermic reactions taking place at temperatures between 661^0C and 801^0C. The decomposition in this range is also attributed to the presence of amorphous calcium carbonate, which decomposes from calcium carbonate to CaO. Calcium carbonate is decomposed with increasing temperature from 801^0C to form CaO. From 801^0C, the amount of CaO is increased, as observed in the TGA curve.

3.2 Consistency on blended cement

The amount of water of control (0 CNSA) and CNSA-blended cement pastes for the attainment of consistency are presented in Fig. 14. The water required for the standard consistency of these cement is substantially enhanced to 57% with the incorporation of CNSA. The consistency of 0 CNSA was found to be 28%, while the same for 5 CNSA, 10 CNSA, 15 CNSA, 20 CNSA, and 25 CNSA was measured to be 34, 39, 41, 42, and 44%, respectively. It is observed from the results that there was an enhancement in the consistency of the cement pastes. This increase in the amount of water required for consistency is potentially due to the greater specific surface of the CNSA particles. Similar results on using agricultural waste leftover ashes have divulged the increased water demand for preparing the cement pastes [65, 66]. With the incorporation of natural and artificial pozzolans having coarser particles than that of OPC [67], the consistency of blended cement diminishes, and an increase in the amount of water was noticed in the subsistence of finer-sized biomass ash [30]. A similar phenomenon was also observed in cement pastes with fly ash blended with a high LOI. [68].

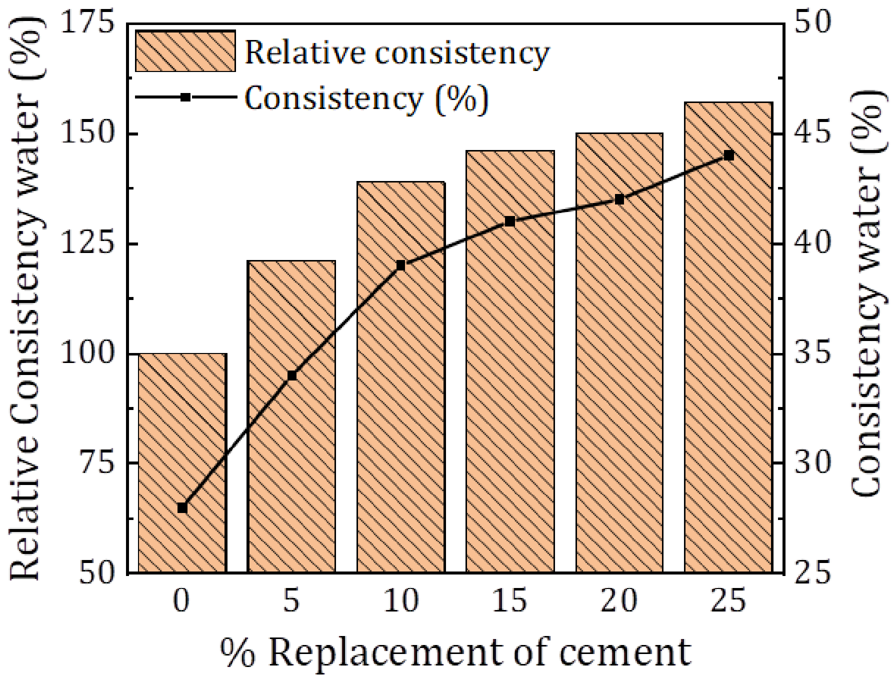

Fig. 14: Consistency of blended cement at different CNSA percentages

3.3 Vicat setting time on blended cement

Initial setting time and Final setting time of the blended cement are presented as shown in Fig. 15. Increase in CNSA percentage subsides the IST and FST of cement pastes. A considerable decrease of 74% and 60% was found in the IST and FST of cement at 5% of CNSA. At higher CNSA replacement levels, the reduction was also seen but relatively in less amount. The incorporation of 25% of CNSA reduced the setting time of cement by 90% and 83%, respectively. An increase in CNSA dosage reduces the IST and FST of cement pastes, signifying that CNSA in cement paste has an accelerating effect. Shorter setting times are achieved due to the accelerating effect of finer mineral admixture particles. The setting is an outcome of the hydration process. Faster the setting indicates that the subsistence of CNSA particles provides supplemental sites for the deposition of hydration products resulting in early hydration of cement [69]. To suppress early hydration problems, the use of special chemical activators such as nano- SiO_2 [70], nano-TiO_2 [71], and graphene oxide [72] has been the nucleus of the latest studies. Thus, CNSA, a fine-grained waste accelerator, can promote the preceding challenges with eco-efficient benefits.

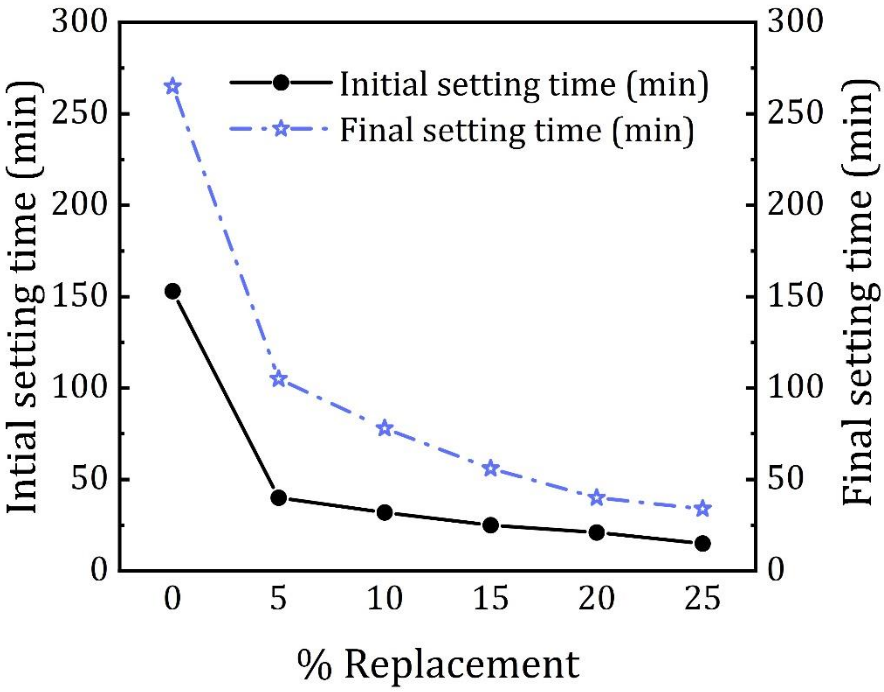

Fig. 15: Setting time of blended cement at different CNSA percentages

3.4 Expansion test on blended cement

The expansion (soundness) is evaluated to divulge the resistance against the volume changes of cement. The expansion of CNSA blended cement is conducted with the aid of the Le Chatelier apparatus for free CaO content. Table 5 shows the influence of the supplements of CNSA in cement paste on the expansion. It is seen that with the addition of CNSA content, the expansion will increase. Compared to cement paste containing CNSA, the control paste showed lower expansion. However, the results indicated that the expansions in all the mixes are under the limit designated by EN 197-1 [73].

Table 5: Expansion of blended cement pastes

Property	Cashew nutshell ash (%)						EN 197-1 Limit
	0 CNSA	5 CNSA	10 CNSA	15 CNSA	20 CNSA	25 CNSA	
Expansion, mm	0.50	1.10	1.50	2.0	2.0	4.5	≤10

3.5 Mini slump tests on blended cement

High mobility and moderate viscosity are essential for the forming of cement-based materials. A mini-slump test was performed due to the limited quantity of cement paste that could be effectuated to measure the workability. Fig. 16 illustrates pictures of the flow of the blended paste at different CNSA percentages. There was no sign of bleeding in any of these mixes. The mini-slump diameter of the cement paste is approximately 92 mm at 0 min, and it is increased to 107 mm at the end of 5 min, yielding a slump of 14%, and reduced to 95 mm at 15 min. However, for the 0 CNSA, the mini-slump value is increased for 2 min and 5 min. For 5 CNSA, the mini-slump values are increased by 6% and 17% at 2 min and 5 min and decreased by 2% and 6% at 10 min and 15 min due to the less mass of CNSA in the mix leading to similar results to 0 CNSA. Results show that the addition of CNSA causes reductions in mini-slump values for 10 CNSA, 15 CNSA, 20 CNSA, and 25 CNSA. Identical trends were observed at all times for all the mixtures mentioned above. Fig. 17 shows the variation of mini-slump flow for the pastes with different percentages of CNSA. Finer particle size has a considerable effect on the flow. This can be due to the high specific surface area that decreases the fresh mix's available water [74, 75]. Also, higher alkali content in CNSA accelerates the hydration thereby affecting the flowability for the higher percentages of CNSA [76] [77].

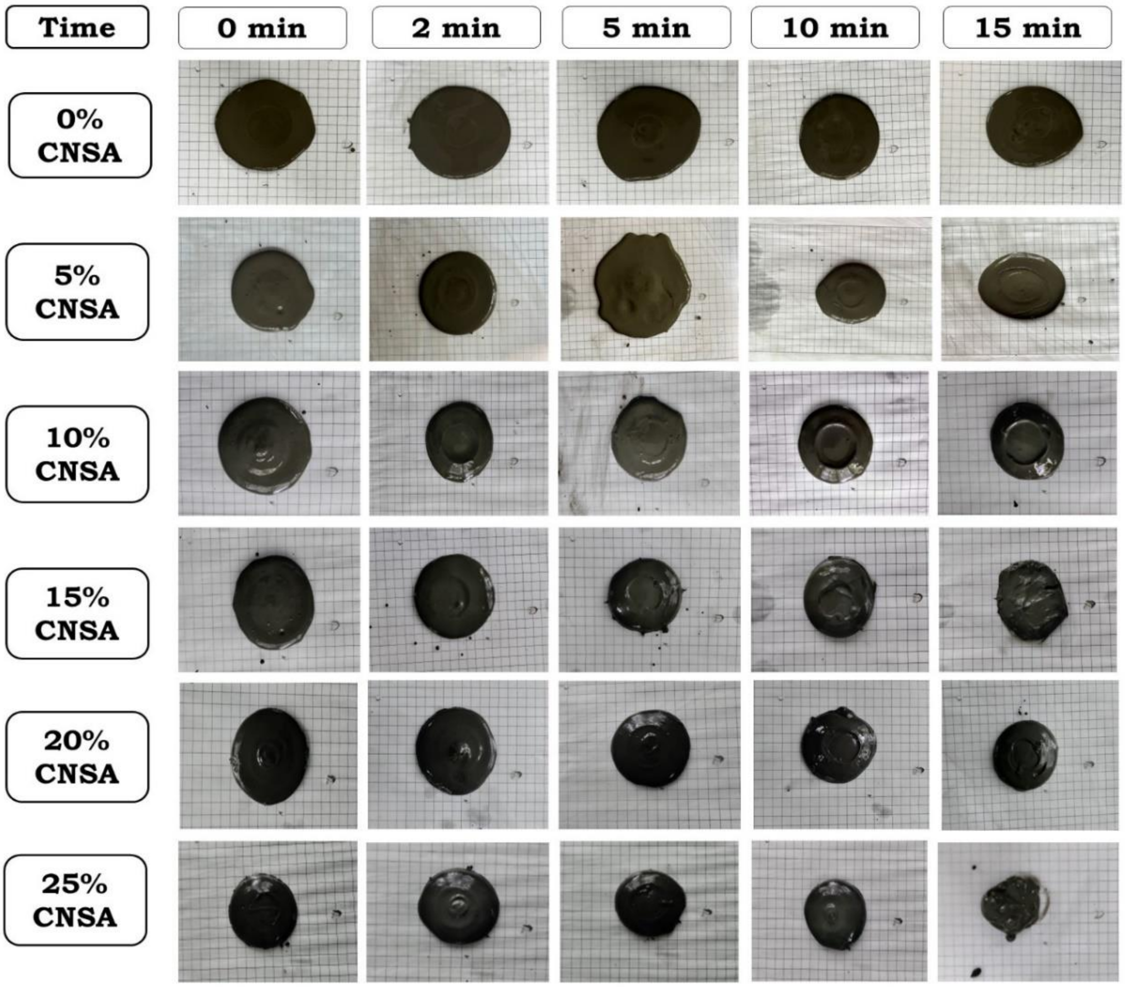

Fig. 16: Pictures of the mini-slump flow of the blended paste at different CNSA percentages

499

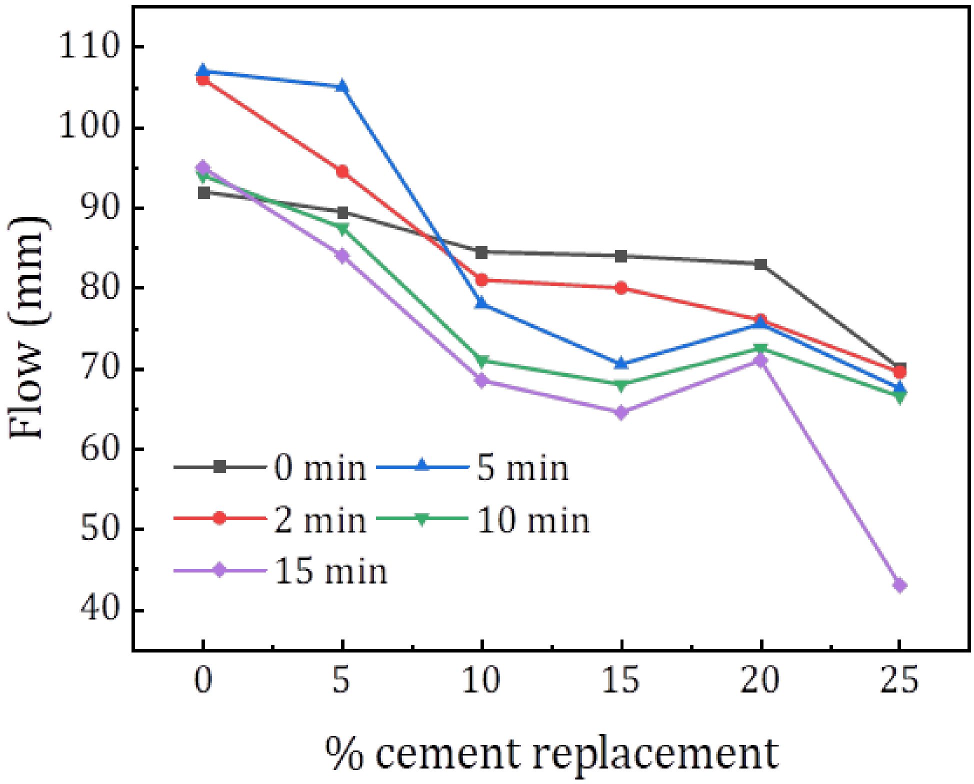

Fig. 17: Mini slump flow of the blended paste at different CNSA percentages

3.6 Flow table test of blended cement

Flow table test was performed on all the mortar mixes incorporating different percentages of CNSA to study the flow properties of the mixes. The test results are exhibited in Table 6 and Fig. 18 presents the flow behaviour with an increase in the percentage of CNSA. Incorporating CNSA into mortar has a noticeable effect on workability. It was observed that the flow value for the CNSA-based cement mortars reduced with an increase in the proportion of CNSA. The 0 CNSA has a flow value of 152 mm. The flow value of mixes 5 CNSA, 10 CNSA, 15 CNSA, 20 CNSA, and 25 CNSA indicate lower values of 141, 138, 137, 128, and 125 mm, respectively. Compared to OPC, CNSA requires extra water because of its irregular shape, excessive porous texture, and angular particle geometry, as seen in the SEM image, which causes a decline in the blended mixes' flow properties. This led to poor workability. As the percentage of agricultural residue ashes increases, its workability decreases [78]. In addition, the high specific surface area of CNSA reduces workability by adding substitution levels. As a result, more water was required to moisten the surface [79].

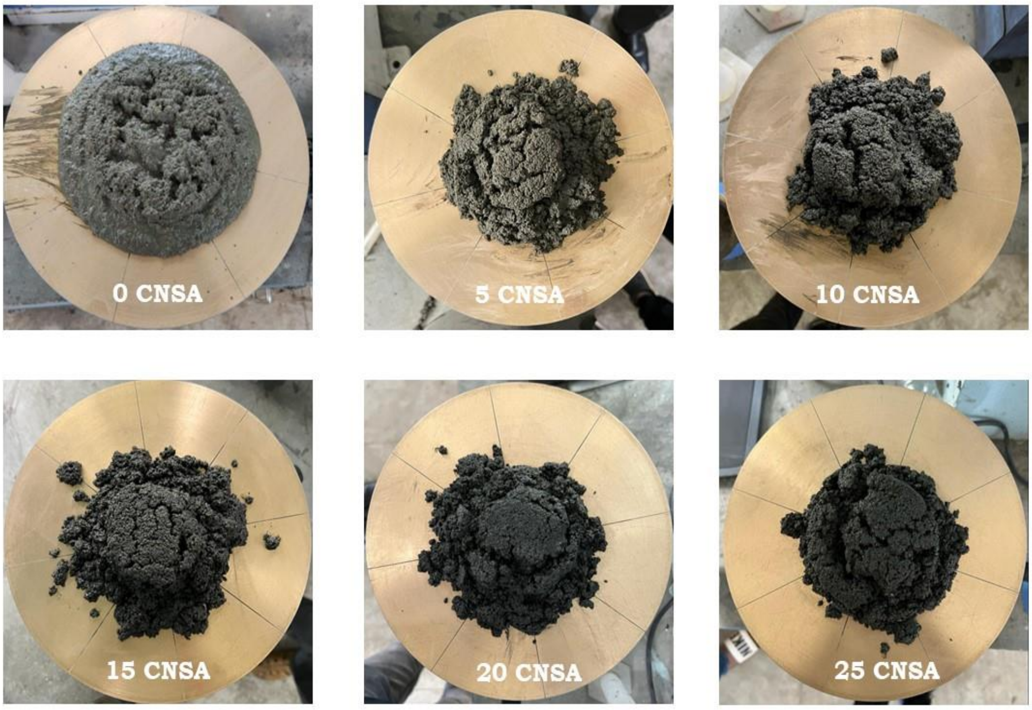

Fig. 18: Pictures of the behaviour of flow at different CNSA percentages

Table 6: Flow table values of Blended cement mortar at different CNSA percentages

Mix	Flow value (mm)
0 CNSA	152
5 CNSA	141
10 CNSA	138
15 CNSA	137
20 CNSA	128
25 CNSA	125

3.7 Hardened properties of blended cement

Fig. 19 enunciates the compressive strength test results of all the mortar mixes at 1, 3, 7, and 28 curing ages. The compressive strength values for 0CNSA, 5CNSA, 10CNSA, 15CNSA, 20CNSA, and 25CNSA are 6.64, 9.14, 10.09, 9.79, 9.11, and 8.26 MPa after one day of curing age. The improvement in 1-day compressive strength is 37.7, 52, 47.4, 37.2, and 24.4%, respectively. Similarly, the compressive strength values for 0 CNSA, 5 CNSA, 10 CNSA, 15 CNSA, and 20 CNSA are 38.96, 33.54, 30.87, 28.73, 24.42, and 21.41 Mpa after 28 days of curing. The decrement in 28-day compressive strength is 13.9, 20.8, 26.3, 37.3, and 45%, respectively. Additionally, the incorporation of higher biomass ash in cement mortars endured an excessive reduction in compressive strength values [80].

In contrast with the control mortar, the blended mortar shows higher compressive strength at an early age. In CNSA, K_2O has a chemical composition of about 52%, much greater than other industrial residues (fly ash, slag, and silica fume). Due to the high alkaline content in CNSA, the addition of CNSA at increasing levels will result in a more alkaline environment than the control mix, resulting in accelerated hydration at early ages and improving early-age strength [77, 81]. In this study, researchers found that the strength values decreased with enhancements in CNSA levels at 28 days as the greater alkali content suppresses hydration at later ages [82]. Also, due to the fact that the high specific surface area of CNSA requires more water to maintain workability, resulting in fewer hydrated CNSA products, thereby reducing compressive strength at 28 days. With higher levels of CNSA in the mortar, 28-day compressive strength was significantly decreased. Fig.20 and Fig.21 indicates the SEM of 10% CNSA at 1 day and 3 days respectively.

Similar findings were identified when the incorporation of the ground nut shell ash [83], untreated corn cob ash [24], and corn stalk ash [81] was used as a cementitious material. High alkali oxide content substantially diminished the compressive strength of the concrete due to an enormous amount of alkali induced into a sulphate disproportion which has an anti-positive impact on the cement hydration.

The CNSA-blended mortar has a lower compressive strength and is most appropriate for applications that do not demand a greater compressive strength. In accordance with ASTM C270 [84], type M, S, and N mortars should have a minimum compressive strength of 17.2, 12.4, and 5.2 MPa after 28 days, respectively. Compressive strength of 21.41 MPa was obtained for 25 CNSA at 28 days. The compressive strength of different mixes was found within the standard value. Also, ASTM C90 [85] requires a minimal compressive strength of 13.8 MPa for load-bearing masonry units that are laid in mortar, which is attainable with the addition of CNSA in the mortar mixture.

According to the strength results, untreated CNSA should not be used as an SCM since it contains high K_2O, P_2O_5, MgO, and high LOI, which reduce the concrete's strength significantly. In one of the research work, it was found that both water and acid washing of the ash showed positive effects on concrete and enhanced the compressive strength at later ages [86]. Although there is no research on the pre-treatment for CNSA, it was hypothesized that the pre-treatment of CNSA could enhance the quality of the ash, decrease the K_2O, and improves its strength.

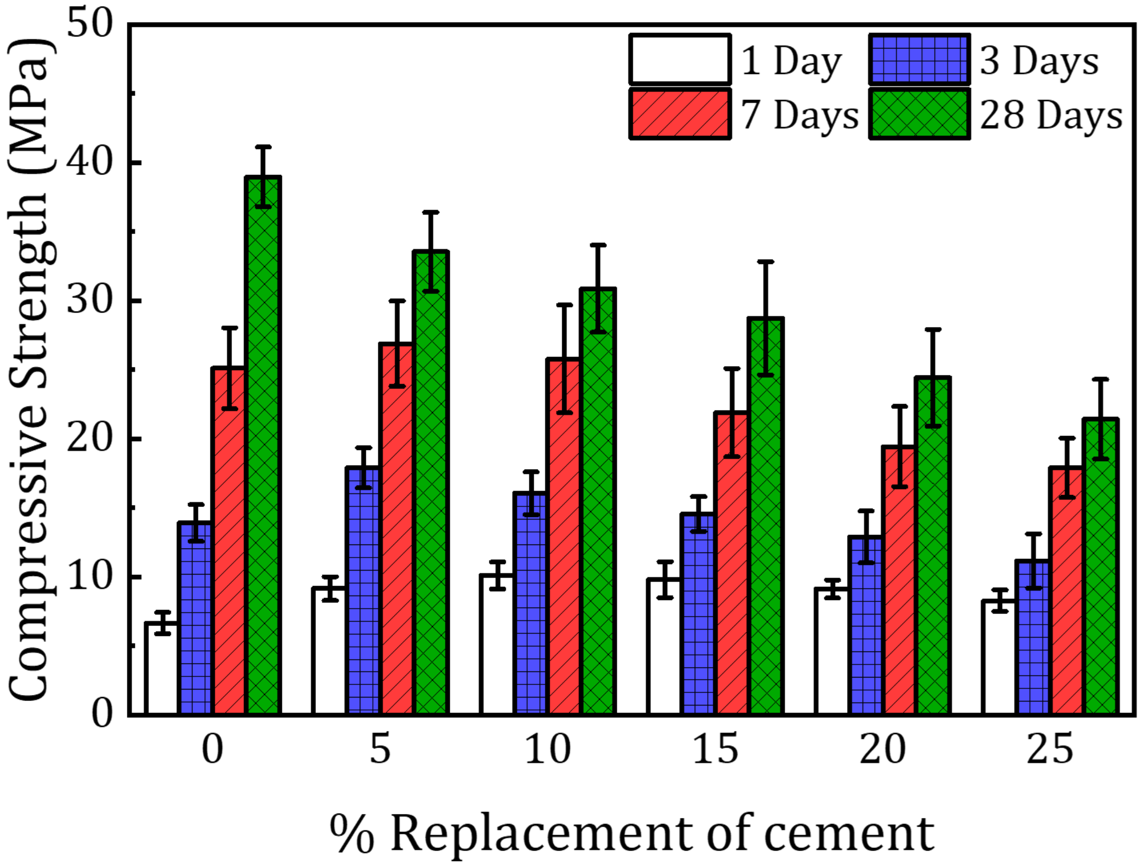

Fig. 19: Compressive strength of Blended cement Mortar at different CNSA percentages

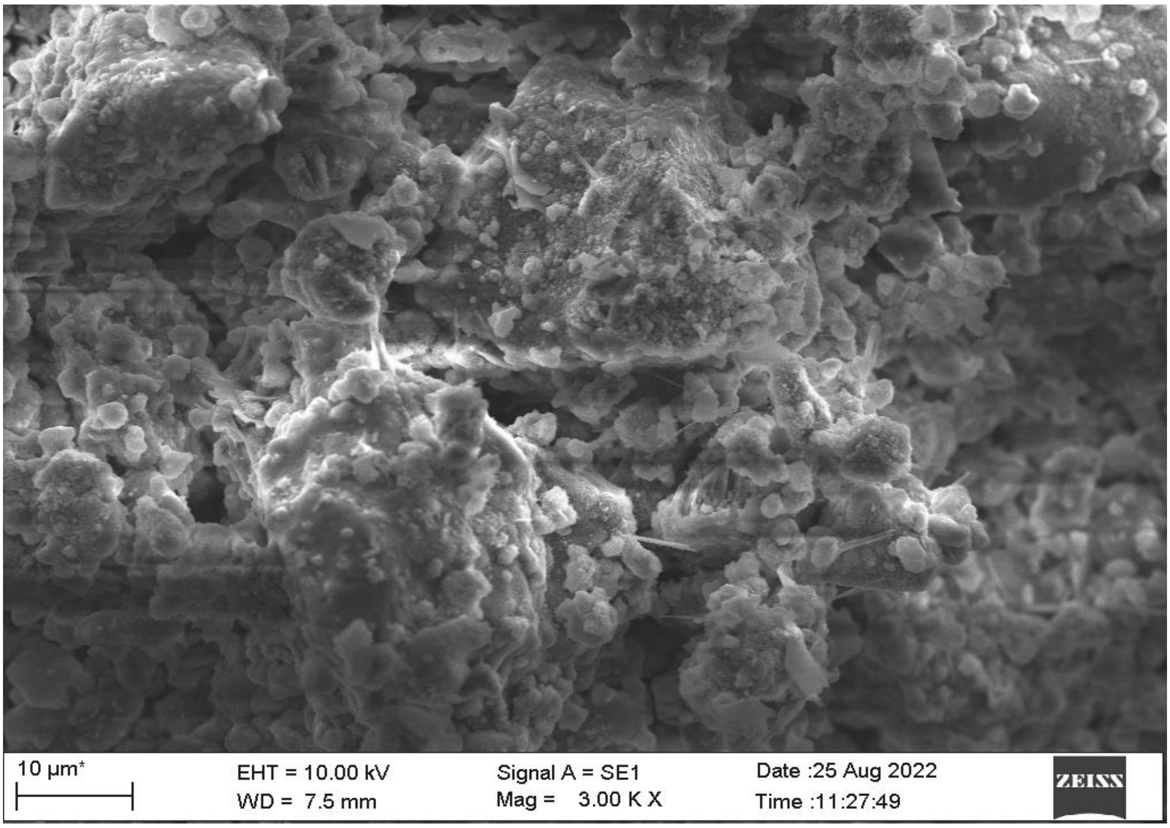

Fig. 20: SEM image of 10% CNSA blended paste at 1 day

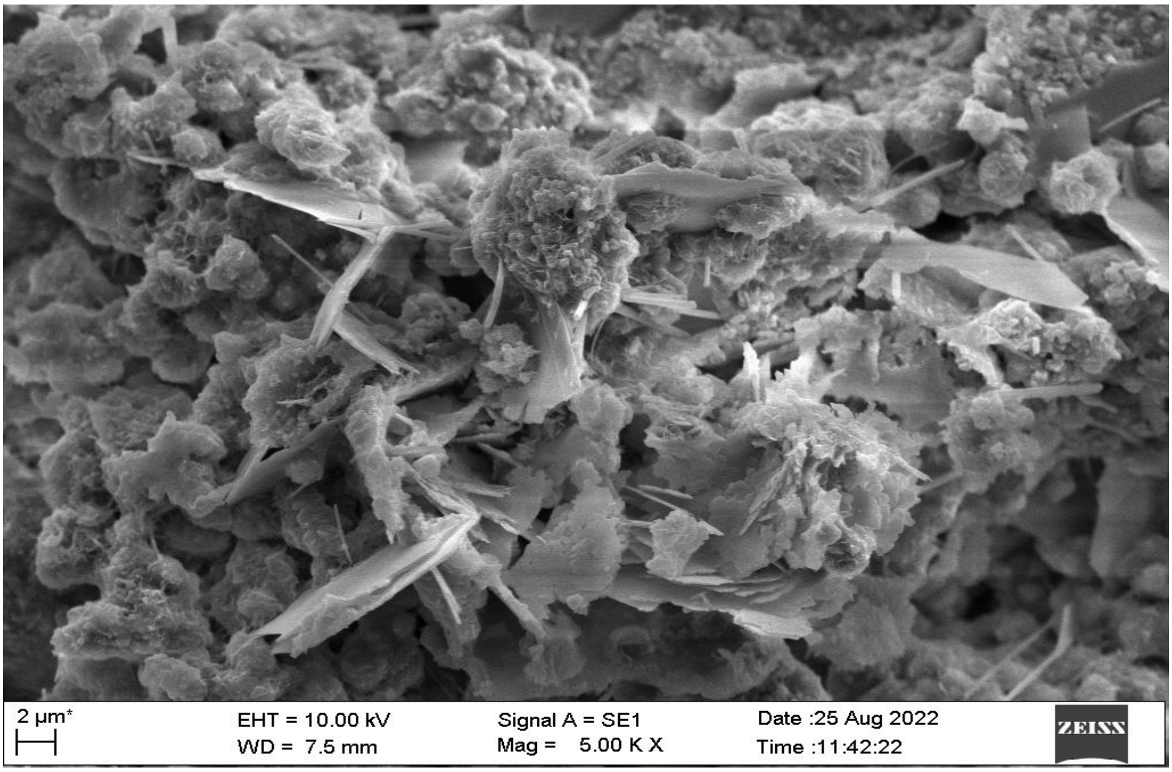

Fig. 21: SEM image of 10% CNSA blended paste at 3 days

3.8 Ultrasonic Pulse velocity

Ultrasonic Pulse Velocity (UPV) is a non-destructive technique for examining concrete for homogeneity and uniformity, voids, and cracks. In UPV, ultrasonic pulses pass-through construction materials are measured to determine their durable properties and hardened strength. UPV values are significantly influenced by pore structure, material properties, mix proportions, and the interfacial zone between aggregates and cement paste [87]. The UPV test results for the CNSA-based blended mortar and OPC mortar are presented in Fig. 22. All the specimens containing different proportions of CNSA were measured for UPV at 7 and 28 days. The UPV values for CNSA-based blended mortar vary from 3535 to 3889 m/s and 3735 to 4465 m/s after 7 and 28 days of curing, and that of OPC is 3889 and 4465 m/s for 7 and 28 days. UPV values of control mortar (0 CNSA) exhibiting dense and compact structure.

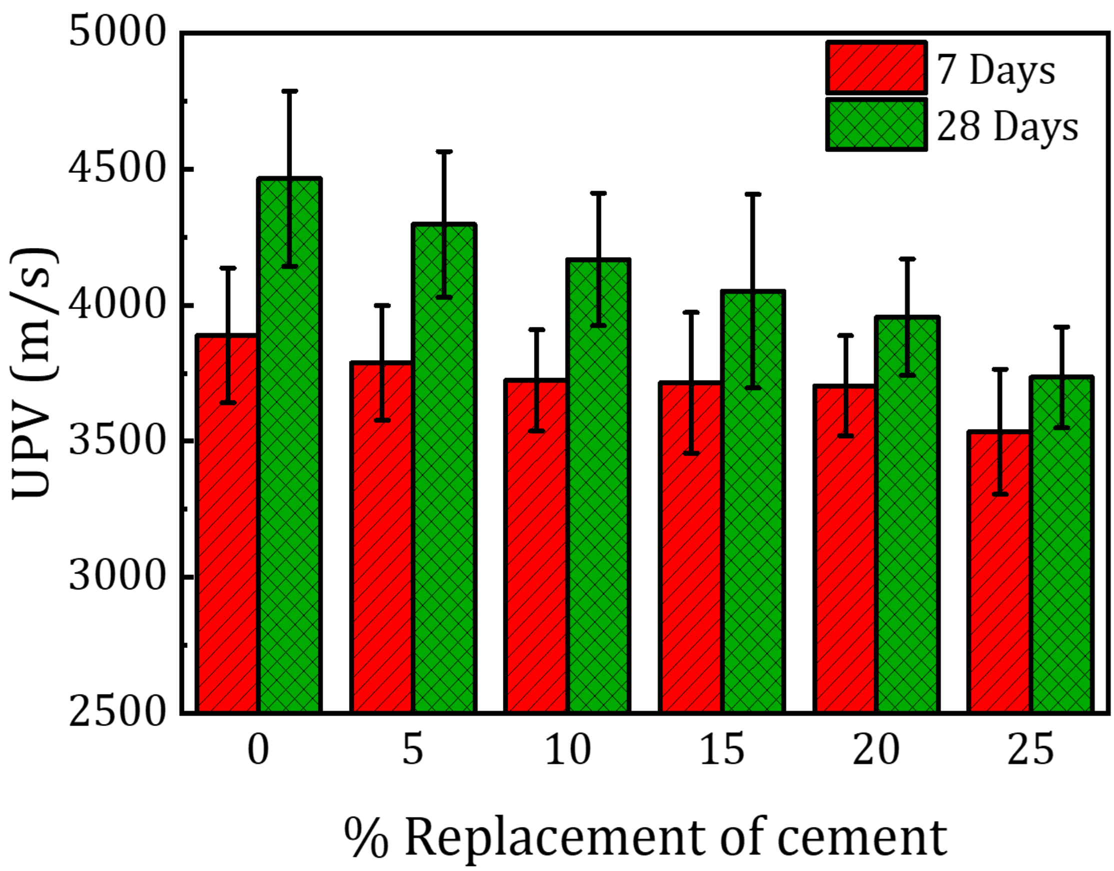

Fig. 22: UPV Values of Blended cement Mortar at different CNSA percentages

The UPV values of all the control mortar and CNSA-based blended mortar specimens increased with the curing period. The compressive strength of all the mortar samples also emanates a similar trend. With increase in CNSA levels, UPV values for 7 and 28 days decreased by 2.59%, 4.24%, 4.47%, 4.75%, 9.10% and 3.76%, 6.65%, 9.24%, 11.39%, 16.34%. Higher the

UPV values, finer will be the quality of cement composites. All the mixes in this study showed UPV values over 3500 m/s. Concrete with pulse velocity values over 3500 m/s stipulates good durability [88] as indicated in Table 7. Therefore, CNSA-based mortars can be classified as durable mortars. This research showed that the mortar has become more condensed with the increase in curing age, so the rationale for high velocity.

Table 7: Quality class achieved by OPC mortar [89-92]

Concrete Quality [89-92]	UPV Range (m/s)
Excellent	>4500
Good	3600 - 4500
Questionable	3000 - 3600
Poor	2100 - 3000
Very Poor	1800 - 2100
Significant abnormality has to be anticipated inside the structure	<1800

3.9 Water absorption, Bulk density (dry), porosity

The water absorption, bulk density, and porosity of mortar with different CNSA contents are shown in Table 8. After 28 days of curing, the absorption of water is calculated to be 5.53, 6.48, 7.13, 8.61, 10.25, and 11.63% for 0 CNSA, 5 CNSA, 10 CNSA, 15 CNSA, 20 CNSA, and 25 CNSA. The increase in water absorption is 17, 29, 55, 85, and 110 %, respectively, correlated to the control mortar. An important factor influencing the water absorption of mortar samples is the formation of the pore system [93]. By observing through SEM, CNSA contains a large number of pores, which can substantially enhance the water absorption of mortar samples as its percentage increases. A possible explanation is that the excess CNSA lacks adequate calcium hydroxide to react with, thus causing pores to form in the mixture, which has caused to absorb more water.

For the above-mentioned mortar mixtures, the porosity value are 7.67, 10.51, 11.37, 13.36, 17.05, 21.31% respectively. Directly obtained biomass ash has asymmetrical shapes, bigger particle sizes, and rough surfaces, leading to high porosity [94]. Blended mortar consists of coarser CNSA particles, which results in the development of more pores. Due to high pores in CNSA, the absorbed water evaporates from the mortar sample during drying. As a result, voids are created in the mortar samples, which will surge the porosity of the mortar. An increase in the porosity results in weaker bonding between particles, which results in lesser compressive strength [95].

Table 8: Water absorption, Bulk density, and Porosity of Blended cement mortar at different CNSA percentages

Mix ID	Absorption after immersion	Bulk density, dry	Porosity
0 CNSA	5.53	2.16	7.67
5 CNSA	6.48	2.15	10.51
10 CNSA	7.13	2.11	11.37
15 CNSA	8.61	2.08	13.36
20 CNSA	10.25	2.02	17.05
25 CNSA	11.63	2.00	21.31

Table 8 exhibits the density of mortar with variations in CNSA content at 28 days. The density of the sample with CNSA was lesser than that of conventional mortar. Compared with conventional mortar, the CNSA-based mortar showed moderately less bulk. 25 CNSA-blended mortar mix showed a 7.24% lower reduction than the control mix due to coarser particles of CNSA than the cement particles. As illustrated in Table 1, CNSA has less SiO_2, thereby, the amount of developed hydration products was lower in CNSA-blended mortar than in the control mortar. High pores in CNSA lead to the reduction in the density of the CNSA-based mortar mixes.

3.10 Electrical resistivity

One of the cementitious mixtures' most essential durability factors is their electrical resistivity. A mortar's electrical resistivity is indirectly proportional to the corrosion rate of metallic embedment. Fig. 23 illustrates the electrical resistivity (ER) for all the control and blended mortar mixes. The 7-day ER value for 0 CNSA is 24547 Ω-cm, increasing to 44125 Ω-cm at 28 days. After 7 days of curing, the ER values for 5 CNSA, 10 CNSA, 15 CNSA, 20 CNSA, and 25 CNSA are measured to be 22737, 22171, 20361, 18089, and 14479 Ω-cm, respectively. For the same mixes, the ER values reach 42571, 41724, 35864, 30005, and 26969 Ω-cm after 28 days, respectively. Nevertheless, with the increase in CNSA substitution levels, the resistivity dramatically decreased by 3.52%, 5.44%, 18.72%, 32%, and 38.8% at 28 days. The more CNSA was replaced with OPC, the porosities presented in mortar were increased, leading to lower ER values. Also, due to the factuality that the CNSA is abundant in potassium, as potassium dissolves in the pore solution, the conductivity of the pore solution increases and decreases the resistivity of concrete [24]. Corrosion is less expected when ER of concrete is equal to or greater than 10000 Ω-cm [96]. ACI Committee 222 [97] recommended limits for corrosion through mortars shown in Table 9. From the above results, we can conclude that all the mixtures with CNSA have a low probability of corrosion at all ages.

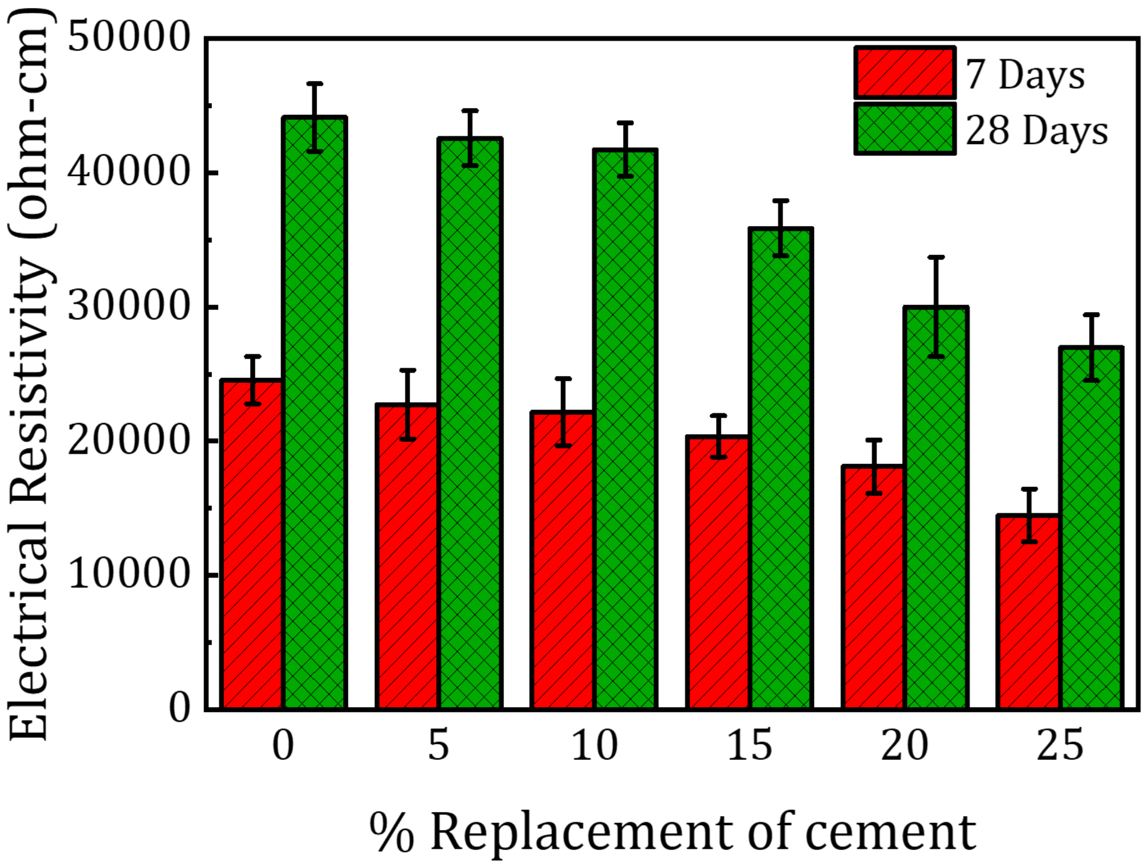

Fig. 23: Electrical resistivity of Blended cement Mortar at different CNSA percentages

Table 9: Resistivity values and risk of corrosion of reinforcement bars [97-99]

Resistivity (Ω-cm)	Corrosion rate
>20000	Low
10000 – 20000	Low to Moderate
5000 – 10000	High
<5000	Very high

3.11 Indices of Pozzolanic effect

Few researchers have previously quantified the pozzolanic effect of active minerals in a mortar [55, 100, 101]. A mineral admixture supplement to concrete or mortar, where its strength is considered in two parts, one from cement hydration and the other from its pozzolanic effect. As per previous studies, pozzolanic effects of CNSA as a cement substitute in mortar were quantified using strength indices [55].

The specific strength ratio is expressed as

$$R = f / q \quad (4)$$

Where f is concrete compressive strength, q is the cement or mineral admixture percentage of the cementitious materials.

R_C articulates the influence of unit cement on concrete strength without any mineral admixture, while R_M divulges the impact of the unit mineral admixture on concrete strength, and R_P is the contribution of the pozzolanic effect to concrete strength due to the mineral admixture, expressed by the equation:

$$R_P = R_M - R_C \quad (5)$$

Index of specific strength (K), K is the ratio of R_M to R_C, and the formula can estimate it:

$$K = R_M / R_C \quad (6)$$

Contribution of pozzolanic effect to strength (P), P is the percentage value of the contribution of the pozzolanic effect to concrete strength, and it can be written as:

$$P = (R_P / R_M) \times 100\% \quad (7)$$

Table 10 shows the influence of CNSA on indices of strength parameters (R_C, R_M, R_P, K, P) at 1,3, 7, and 28 days for all mortar mixes. Fig. 24 illustrates that the P value is increased for all the percentages of CNSA at 1 day because higher alkali content (K_2O and Na_2O) accelerates the cement hydration at an early age. The value of P indicates that the addition of CNSA has positive pozzolanic effects on mortar strength at 1 day. At 3 days value of P is higher than the amount of CNSA, up to 5%, 10%, and 15%, respectively. However, the P value is positive for 20% CNSA and 25% CNSA but is lesser than the amount of CNSA added to the mix, showing the minor pozzolanic contribution to strength.

Similarly, at 7 days, the value of P is higher than the amount of CNSA, up to 5% and 10%, respectively. For 20% CNSA and 25% CNSA, the value of P is negative showing minimum contribution to the strength. These results are associated with the compressive strength test results, where all the CNSA mixes achieved lesser compressive strength than the control mortar at 28 days because the alkali content in CNSA contributes to the degradation of mortar compressive strength over time [82]. Therefore, the value of P for all the CNSA blended mixes at 28 days was negative, indicating less contribution for pozzolanicity at later ages. This study showed that the CNSA could be used for the application where early strength development is required.

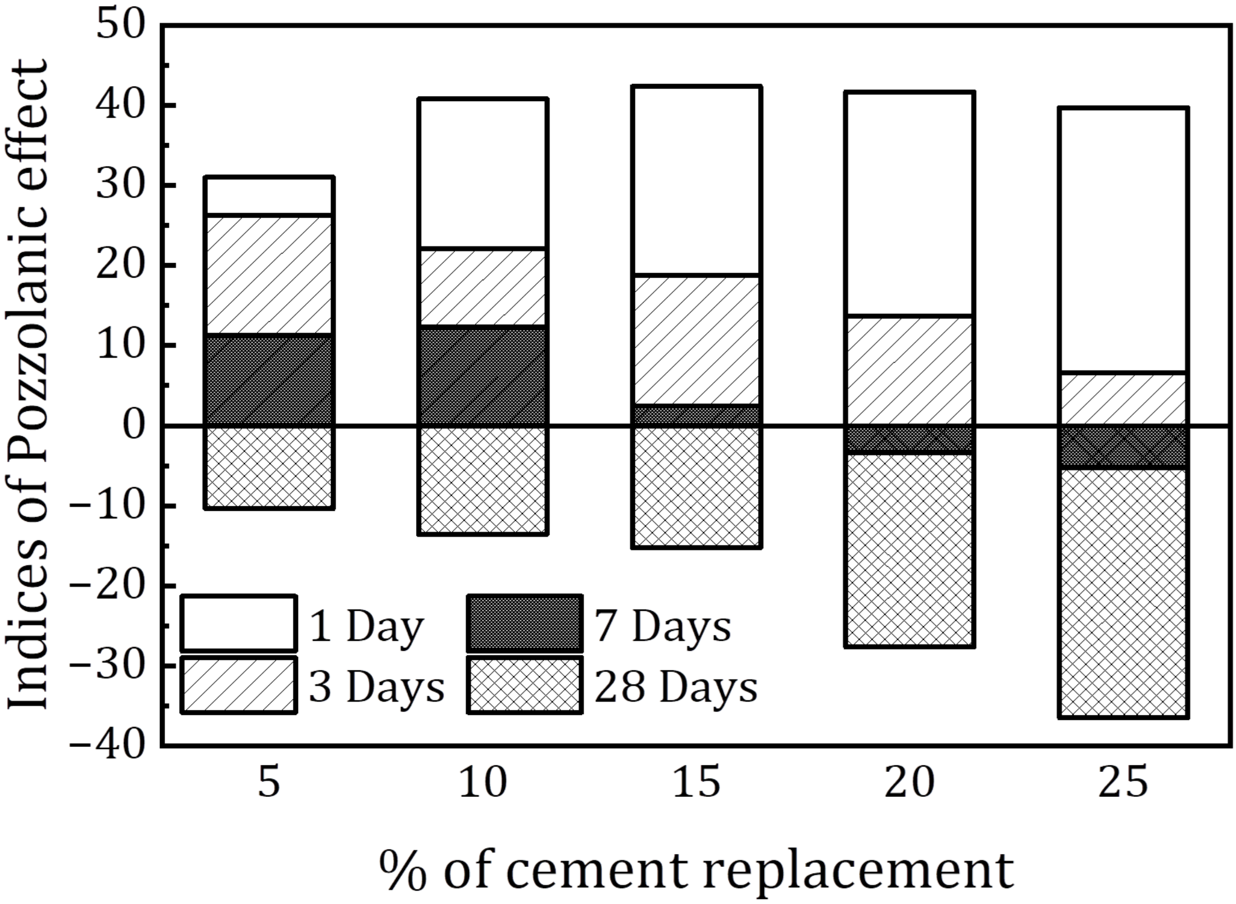

Fig. 24: Pozzolanic effect of Blended cement Mortar at different CNSA percentages

Table 10: Strength index parameter of mortar

Mix ID	q (%)	R_M				R_P				K				P			
		1 day	3 days	7 days	28 days	1 day	3 days	7 days	28 days	1 day	3 days	7 days	28 days	1 day	3 days	7 days	28 days
0 CNSA	100	0.07	0.14	0.25	0.38	0	0	0	0	1	1	1	1	0	0	0	0
5 CNSA	95	0.10	0.19	0.28	0.35	0.029	0.049	0.031	-0.036	1.44	1.35	1.12	0.90	30.98	26.24	11.28	-10.35
10 CNSA	90	0.11	0.18	0.29	0.34	0.045	0.039	0.035	-0.046	1.68	1.28	1.14	0.88	40.77	22.11	12.33	-13.58
15 CNSA	85	0.12	0.17	0.26	0.33	0.048	0.032	0.0064	-0.051	1.73	1.23	1.02	0.86	42.34	18.79	2.49	-15.26
20 CNSA	80	0.11	0.16	0.24	0.30	0.047	0.022	-0.008	-0.084	1.71	1.15	0.95	0.78	41.69	13.72	-3.38	-27.63
25 CNSA	75	0.11	0.15	0.24	0.28	0.043	0.009	-0.012	-0.104	1.65	1.07	0.94	0.73	39.70	6.56	-5.26	-36.47

4. Sustainability and cost assessment

4.1 CO_2 Emissions

The corresponding CO_2 emission values for OPC [102], water [103], and fine aggregates [103] were taken from the literature. Embodied carbon of CNSA is not available in the literature, so the embodied carbon used is subject to certain presumptions. In the present study, only the carbon emissions caused by the transportation and processing of CNSA are considered since the cashew nut industry burns CNS as fuel. For CNSA, the CO_2 emissions were calculated according to the method described by [104]. CNSA is collected from Kalbhavi Industries, Mangaluru; The distance between the cashew industry and the laboratory where the casting and testing were done is roughly 35 km.

Multi-Utility Vehicle (MUV) capacity of 1000 kg was used to transport the CNSA. The electricity consumed for oven drying CNSA for 24 hours at 105°C is at a rate of 1041.67 W/h [104]. Furthermore, assuming that to process (Drying, pulverizing, and Ball milling) the 1000 kg CNSA, approximately 174.7 kWh electricity will be consumed (considering the same as Pulverized Oil Fuel Ash) [104]. According to CO_2 Baseline Database for the Indian Power Sector, October 2021 [105], the CO_2 emission factor for each kilowatt-hour of electricity consumed is 0.79 $kgCO_2/kWh$, while 0.145 $kgCO_2/km$ emission factors for MUV as per India Specific Road Transport Emission Factors [106]. Using these emission factor values, 1 kg of CNSA has an embodied carbon of 0.143 kg.

Table 11: CO_2 emission factors for the primary ingredients used in all the mortar mixes

Cement	Sand	Water	CNSA
0.82 [102]	0.024 [103]	0.0013 [103]	0.143 (Table 13)

Control and CNSA-based mortar production were used to calculate the embodied GHGE ECO_2e and the embodied energy EE for 1 kg of each Type of mortar using Eq.8, 9 [95]

$$ECO_2e = \Sigma\, CO_{2i} \times m_i \quad (8)$$

$$EE = \Sigma\, E_i \times m_i \quad (9)$$

CO_{2i} is the embodied carbon factors, E_i is the embodied energy factors per unit mass of constituent i, and m_i corresponds to the mass of mortar ingredient i per kg of mortar.

The EE to produce raw materials is obtained from various sources detailed in Table 12.

Table 12: Embodied energy for the ingredients used in all the mortar mixes

Cement	Sand	Water	CNSA
5.5 [107]	0.34 [103]	0.0017 [103]	2.21

Table 13: CO_2 emission factors for CNSA

Sl No	Item	Energy requirements for 1000 kg of CNSA			Transportation of 1000 kg of CNSA		Total emission ($kg\ CO_2/kg$ CNSA)
		Consumption (kWh)		Emission factor ($kg\ CO_2/kWh$)[3]	Distance (km)[4]	Emission factor ($kg\ CO_2/km$)[5]	
		Drying[1]	Pulverizing and Ball milling[2]				
1	CNSA	25 [104]	149.7 [104]	0.79	35	0.148	0.143

[1] A 1041.67 W/h consumption rate was observed from the oven during 24 hours of drying [104]

[2] Energy engrossed by Pulverizing and Ball milling machines [104]

[3] Emission factors due to the development of electricity [105]

[4] Distance from the cashew nut industry to the laboratory

[5] Emission factor of the MUV used to transport the materials [106]

Moreover, the production of CNSA is involved in transporting, drying, pulverizing, and ball milling. However, the embodied carbon estimated based on these aspects was 0.143 kgCO_2/kg as seen in Table 11 and Table 13. An investigation by Dissanayake et al. [108] denotes that the utilization of the waste materials results in nearly zero EE, but the EE utilized for transporting, drying, pulverizing, and ball milling is to be considered. As per the greenhouse gas: reporting conversion factor from Department for Business, Energy, and Industrial Strategy, the conversion factors is 0.233 kgCO_2 per kWh [109]. Also, 1 MJ equals 0.2778 kWh [110], and the equivalent carbon dioxide released for the transporting, drying, pulverizing, and ball milling of the CNSA was considered. Hence for CNSA, which was acquired as direct waste, the EE derived as 2.21 MJ/kg. Although there are no values with the CNSA in the literature, this result elucidates the one found for the rice husk ash [111], which is an agro-industrial waste.

Mortar with CNSA in varied proportions as a replacement for cement was evaluated for their environmental efficacy. Compared to control mortar, CNSA mortars contribute less greenhouse gas emissions, making them environmentally friendly. The derived results are illustrated in Fig. 25. It can be divulged that the incorporation of CNSA in mortar led to a substantial decrease in the embodied carbon of the mixes. CNSA incorporation into mortar clearly affects the difference obtained for ECO_2e for different mortars. From Fig.25, it can be revealed that the utilization of CNSA in mortar led to a significant decline in the embodied carbon of the mixture. The embodied carbon of blended mortar is 3.8%, 7.6%, 11.4%, 15.2%, and 19% lesser than that of the control mortar at 5%, 10%, 15%, 20%, and 25% of OPC replaced with CNSA. The mix with the utmost percentage replacement of CNSA emitted the least amount of ECO_2e among the different proportions.

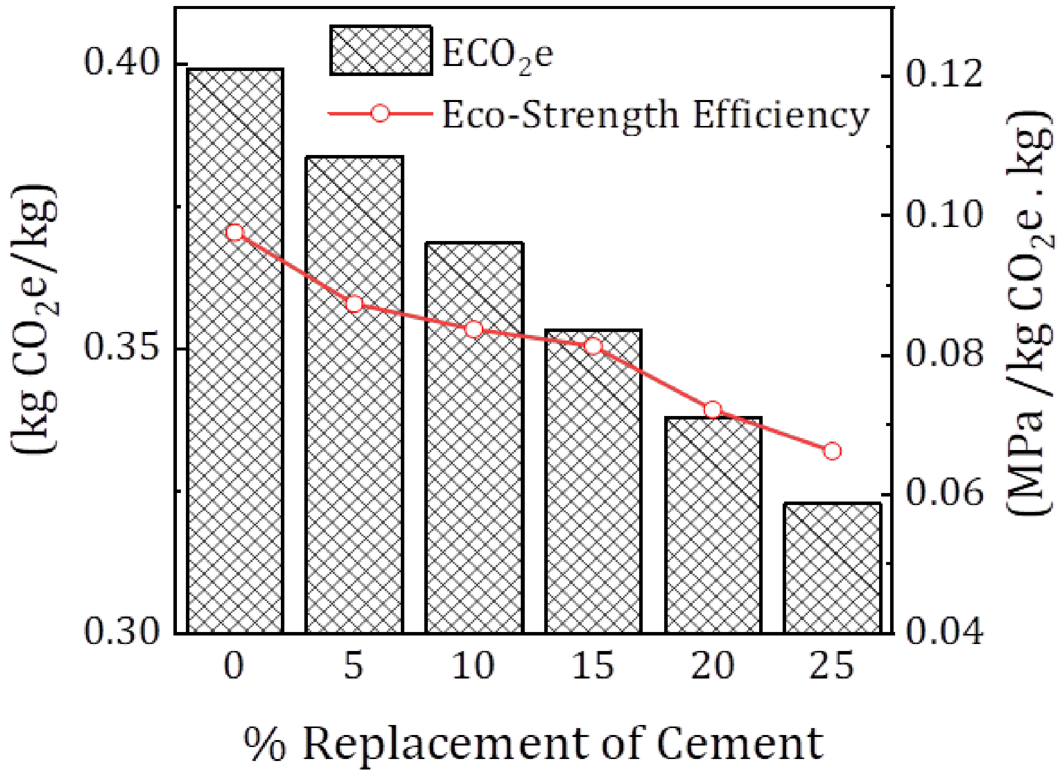

Fig. 25: Embodied carbon and Eco-strength efficiency of Blended cement Mortar at different CNSA percentages

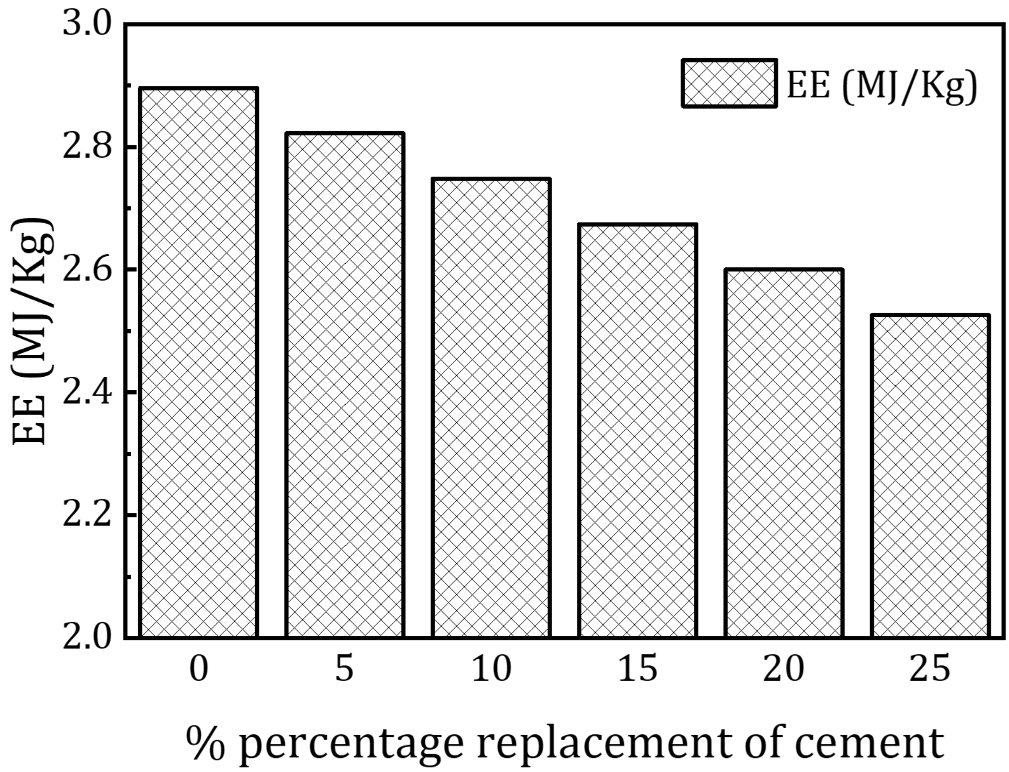

Fig. 26: Embodied energy of Blended cement Mortar at different CNSA percentages

4.2 Embodied Energy

Fig. 26 shows the embodied energy of control mortar and the varying percentages of CNSA. As seen in Fig. 26, the maximum amount of EE is developed by control mortar compared to different mixes. The amount of EE is 2.89, 2.82, 2.74, 2.67, 2.60, 2.52 MJ/kg with 0, 5, 10, 15, 20 and 25% CNSA levels. The reduction of EE is 2.5, 5.1, 7.6, 10.2 and 12.7% compared to control mortar. According to these findings, CNSA fractionally substituted with cement led to a reduction in EE.

4.3 Eco-strength Efficiency

A varied mix of CNSA will result in different total CO_2 emissions. However, it is essential to focus not only on reducing embodied carbon but also on the abatement of materials and the impact on compressive strength [112]. An eco-strength efficiency indicator using Eq. 13 [104] can be used for a better understanding,

$$\text{Eco-strength efficiency} = \frac{\text{Average 28-day compressive strength of mortar}}{\text{Total Embodied carbon of mortar}} \qquad (10)$$

According to Fig.25, the control mortar with 0% CNSA has an efficacy of 0.0976 MPa/kgCO_2e.kg for 28 days. From Fig.25, it can be seen that the eco-strength efficiency of CNSA blended mortar is decreased at all levels compared to control mortar. This can be due to the decrease in compressive strength of all the CNSA blended mortar mixes at 28 days. By substituting OPC with 5%, 10%, 15%, 20%, and 25%, the eco-strength efficiency is lowered by 10.4%, 14.2%, 16.7%, 26%, and 32%, respectively. As mentioned earlier, CNSA blended mortars can be used for applications that do not require high compressive strength. Also, the strength values obtained for CNSA blended mortars were found to be more than the ASTM standards (ASTM C270 and ASTM C90). However, it is essential to focus not only on the reduction of eco-strength efficiency but also on the reduction in the constituents with replacement levels of OPC and embodied carbon.

Despite its meager contribution to reducing CO_2 emissions, CNSA offers the advantage of conservation of natural resources and can be used to develop ecologically beneficial and energy-efficient mortars for the cement industry to promote sustainable growth.

4.4 Cost assessment

The CNSA used in this study is an untreated regional waste material obtained directly from the industry. The ash obtained will be disposed of on land, so the processing cost for CNSA is relatively less than the cement. Therefore, the cost for drying, pulverizing, ball milling, and transporting CNSA will be considered in this study. From table 13, total electricity consumption for drying, pulverizing, and ball milling of 1000kg of CNSA is 174.7 kWh. The cost of 174.7 units consumed for drying, pulverizing, and ball milling of 1000kg of CNSA is Rs. 1398.00* /1000 kg. CNSA of 1000kg transported for a distance of 35 km, the cost for transporting CNSA is Rs. 619.78* /1000 kg. Hence, total cost of CNSA is Rs. 2.017* /kg. To calculate the quantity of cement and sand for 1m^3 of mortar for a mix ratio of 1:2.75, weight of cement and sand is 510.72 kg/m^3 and 1404.48 kg/m^3. Table 14 indicates the total cost of mixes for 1m^3 of mortar

Table 14: Total cost of the mixes for 1m^3 of mortar

Mix	Cement (kg/m^3)	CNSA (kg/m^3)	Sand (kg/m^3)	Total (Rs / m^3)
0 CNSA	510.72	-	1404.48	6192.48
5 CNSA	485.22	25.53	1404.48	6039.97
10 CNSA	459.66	51.06	1404.48	5886.98
15 CNSA	434.13	76.59	1404.48	5734.24
20 CNSA	408.60	102.12	1404.48	5581.49
25 CNSA	383.04	127.68	1404.48	5428.57

* Cost can be varied based on market conditions

Conclusion

3R's - Reducing, recycling, and reusing waste is one of the important goals of the world's sustainability. A country's sustainable development depends on tackling waste materials that cause regional environmental contamination and reusing them for sustainable development. Hence, this study divulged the practicability of harnessing the waste CNSA on the characteristics of the cement pastes and mortars. The CNSA was utilized in developing a mortar mix by substituting the cement at various levels and the fresh and hardened characteristics of paste and mortar is studied. Embodied energy and carbon assessment, eco-strength efficiency were used to assess the sustainability performance of mortars. Based on the results, the following conclusions can be drawn.

- The reactive phases and high specific area of CNSA lead to additional water for attaining the consistency of cement paste.
- CNSA has an acceleration effect on the setting time of blended cement pastes. Due to the presence of high alkali (K_2O and Na_2O) in CNSA, the precipitousness of cement hydrates occurs at a faster rate, leading to a shortening in the induction period and reduction in the setting time of cement pastes.
- Results show that incorporating CNSA in more significant amounts decreases the mini-slump flow of the cement paste. The particle size of CNSA has a substantial influence on the flow.
- The workability of all the mixes of blended mortar is found to be more than 110 mm. Higher the replacement levels, flow values were decreased by 7%, 9%, 10%, 16% and 18% respectively. CNSA particles exhibit more angularity, aggregation and reactive phases, leading to an decrease in flowability.
- CNSA leads to higher compressive strength at an early age as the alkali in cement accelerates the hydration at an early age. At 28 days, the compressive strength of all the replacement levels is 14%, 21%, 26%, 37%, and 45% less than the control mortar. At later ages, the mechanical properties of cement-based materials were adversely affected by the high alkali content in blended cement mortar. However, CNSA-blended mortars can be potentially used in masonry units. The findings of this study shows that regional waste material CNSA can be utilized in smaller amounts.
- Porosity is the main factor influencing the UPV values, and higher porosity negatively affects the UPV. The partial replacement of OPC with CNSA in mortars decreases the UPV

values with an increase in percentage. However, the CNSA blended mortar is in a good quality with UPV of 3500 – 4500 m/s.

- CNSA concrete exhibited a lower bulk density than the control mortar. This is because the specific gravity value of CNSA is lower than that of cement, resulting in a decrease in the bulk density of mortar with CNSA.
- The indices of the pozzolanic effect ‘P’ have positively contributed to the strength during the initial ages. For later ages (at 28day), the value of ‘P’ decreased than the amount of CNSA, indicating negative pozzolanic contribution to the strength.
- The sustainability assessment shows a substantial reduction in the embodied carbon, energy, and overall carbon footprint for all the replacement levels of CNSA. The eco-strength efficiency of CNSA blended mortar was reduced than the control mortar for all the mixes. Also, the cost assessment of the mortar mixes indicated that the CNSA can be used as a cost-effective accelerator.

CNSA as a partial substitute for the cement found to be promising for certain desired characteristics of cement despite its limitations in strength at later ages. CNSA is an underutilized resource that has the potential to evolve as a construction material. A great deal of research is required for CNSA to enhance its efficiency and material's characteristics for construction applications. The present literature mainly focuses on mortar's fresh and mechanical properties utilizing CNSA. However, the effects on reactivity, hydration, microstructure, and durability are yet to be thoroughly studied. Also, researchers may attempt to investigate the possibility of using CNSA on the performance of structural concrete. Further, due to the higher alkali content of CNSA, more research is needed to investigate if this type of ash promotes an alkali-silica reaction.

In addition, this work provides a dual opportunity for the production of CNSA at an industrial scale and to blend with Portland cement. While processing CNSA, industries can adopt suitable methods for sieving and grinding to the desired fineness. The processed CNSA from the cashew industry can be exported to the cement industry and blended with the clinker to make high-quality, sustainable quick accelerating cement. Thus, CNSA can generate substantial income for the industry and be used in cement production as a blended material. However, it is still necessary to conduct a great deal of research on CNSA to prove its suitability for cementitious composites.

Credit authorship contribution statement

Manjunath Balasubramanya: Conceptualization, Idea, Investigation, Data curation, Validation, Formal analysis, Methodology, Visualization, Writing - original draft, Writing - review & editing. **Claudiane M. Ouellet-Plamondon:** Formal analysis, Data curation, Validation, Writing - original draft, Writing - review & editing. **BB Das:** Investigation of TGA. **Chandrasekhar Bhojaraju:** Conceptualization, Investigation Validation, Formal analysis, Methodology, Visualization, Supervision, Resources, Funding acquisition, Writing - review & editing.

Declaration of competing interest

The authors declare that there are no competing interests regarding the publication of this paper.

Acknowledgements

The authors would like to thank St Joseph Engineering College, Mangaluru, Karnataka for their financial support (SJEC/DIR/ST/S/20/20) throughout the research work. The authors would like to thank the technical staff and students for their support in our experiments. The authors are grateful to the National Centre for Earth Science Studies, Thiruvananthapuram for XRF and particle size analyzer facility, National Institute of Technology, Surathkal, Karnataka and Manipal academy of higher education (MAHE), Karnataka for providing help with the XRD, TGA, SEM and EDS facilities.

Data Availability statement

All data, models and code generated or used during the study appear in the published article.

References

[1] C.-Y. Zhang, R. Han, B. Yu, Y.-M. Wei, Accounting process-related CO2 emissions from global cement production under Shared Socioeconomic Pathways, Journal of cleaner production 184 (2018) 451-465.

[2] M.A. Caronge, M. Tjaronge, I.R. Rahim, R. Irmawaty, F.E. Lapian, Feasibility study on the use of processed waste tea ash as cement replacement for sustainable concrete production, Journal of Building Engineering 52 (2022) 104458.

[3] A. Pandey, B. Kumar, Effects of rice straw ash and micro silica on mechanical properties of pavement quality concrete, Journal of Building Engineering 26 (2019) 100889.

[4] S. Sharma, Building a New India, 2018. https://www.kanvic.com/grey-matter/building-a-new-india.

[5] S. Shrivastava, R. Shrivastava, A systematic literature review on green manufacturing concepts in cement industries, International Journal of Quality & Reliability Management (2017).

[6] S. Kenai, W. Soboyejo, A. Soboyejo, Some engineering properties of limestone concrete, Materials and manufacturing processes 19(5) (2004) 949-961.

[7] F. Pacheco-Torgal, J. Labrincha, The future of construction materials research and the seventh UN Millennium Development Goal: A few insights, Construction and building materials 40 (2013) 729-737.

[8] F. Belaïd, How does concrete and cement industry transformation contribute to mitigating climate change challenges?, Resources, Conservation & Recycling Advances 15 (2022) 200084.

[9] R. Isaksson, Process based system models for detecting opportunities and threats–the case of World Cement Production, International Journal of Quality and Service Sciences (2016).

[10] B.S. Thomas, J. Yang, A. Bahurudeen, J.A. Abdalla, R. Hawileh, H.M. Hamada, S. Nazar, V. Jittin, D.K. Ashish, Sugarcane bagasse ash as supplementary cementitious material in concrete–A review, Materials Today Sustainability 15 (2021) 100086.

[11] I. Tekin, İ. Dirikolu, H. Gökçe, A regional supplementary cementitious material for the cement industry: Pistachio shell ash, Journal of Cleaner Production 285 (2021) 124810.

[12] A.A. Amer, S. El-Hoseny, Properties and performance of metakaolin pozzolanic cement pastes, Journal of Thermal Analysis and Calorimetry 129(1) (2017) 33-44.

[13] A. Khan, M.A. Sikandar, M.T. Bashir, S.A.A. Shah, B. Zamin, K. Rehman, Assessment for utilization of tobacco stem ash as a potential supplementary cementitious material in cement-based composites, Journal of Building Engineering 53 (2022) 104531.

[14] V. Brial, H. Tran, L. Sorelli, D. Conciatori, C.M. Ouellet-Plamondon, Evaluation of the reactivity of treated spent pot lining from primary aluminum production as cementitious materials, Resources, Conservation and Recycling 170 (2021) 105584.

[15] K. Scrivener, F. Martirena, S. Bishnoi, S. Maity, Calcined clay limestone cements (LC3), Cement and Concrete Research 114 (2018) 49-56.

[16] R. Snellings, Assessing, understanding and unlocking supplementary cementitious materials, RILEM Technical Letters 1 (2016) 50-55.

[17] S. Kappenthuler, S. Seeger, From resources to research—a framework for identification and prioritization of materials research for sustainable construction, Materials Today Sustainability 7 (2020) 100009.

[18] G. Athira, A. Bahurudeen, V. Vishnu, Availability and accessibility of sugarcane bagasse ash for its utilization in Indian cement plants: A GIS-based network analysis, Sugar Tech 22(6) (2020) 1038-1056.

[19] V. Jittin, A. Bahurudeen, Evaluation of rheological and durability characteristics of sugarcane bagasse ash and rice husk ash based binary and ternary cementitious system, Construction and Building Materials 317 (2022) 125965.
[20] J.B. Jamora, S.E.L. Gudia, A.W. Go, M.B. Giduquio, J.W.A. Orilla, M.E. Loretero, Potential reduction of greenhouse gas emission through the use of sugarcane ash in cement-based industries: A case in the Philippines, Journal of Cleaner Production 239 (2019) 118072.
[21] A.P. Vieira, R.D. Toledo Filho, L.M. Tavares, G.C. Cordeiro, Effect of particle size, porous structure and content of rice husk ash on the hydration process and compressive strength evolution of concrete, Construction and Building Materials 236 (2020) 117553.
[22] N. Chusilp, C. Jaturapitakkul, K. Kiattikomol, Utilization of bagasse ash as a pozzolanic material in concrete, Construction and Building Materials 23(11) (2009) 3352-3358.
[23] M. Moraes, J. Moraes, M. Tashima, J. Akasaki, L. Soriano, M. Borrachero, J. Payá, Production of bamboo leaf ash by auto-combustion for pozzolanic and sustainable use in cementitious matrices, Construction and Building Materials 208 (2019) 369-380.
[24] M. Shakouri, C.L. Exstrom, S. Ramanathan, P. Suraneni, Hydration, strength, and durability of cementitious materials incorporating untreated corn cob ash, Construction and Building Materials 243 (2020) 118171.
[25] T.S.B.A. Manan, N.L.M. Kamal, S. Beddu, T. Khan, D. Mohamad, A. Syamsir, Z. Itam, H. Jusoh, N.A.N. Basri, W.H.M.W. Mohtar, Strength enhancement of concrete using incinerated agricultural waste as supplementary cement materials, Scientific reports 11(1) (2021) 1-12.
[26] K. Wi, H.-S. Lee, S. Lim, H. Song, M.W. Hussin, M.A. Ismail, Use of an agricultural by-product, nano sized Palm Oil Fuel Ash as a supplementary cementitious material, Construction and Building Materials 183 (2018) 139-149.
[27] Y. Lv, G. Ye, G. De Schutter, Characterization of cogeneration generated Napier grass ash and its potential use as SCMs, Materials and Structures 52(4) (2019) 1-12.
[28] F. Cao, H. Qiao, Y. Li, X. Shu, L. Cui, Effect of highland barley straw ash admixture on properties and microstructure of concrete, Construction and Building Materials 315 (2022) 125802.
[29] A. Qudoos, H.G. Kim, J.-S. Ryou, Effect of mechanical processing on the pozzolanic efficiency and the microstructure development of wheat straw ash blended cement composites, Construction and Building Materials 193 (2018) 481-490.
[30] Y. Baran, H. Gökçe, M. Durmaz, Physical and mechanical properties of cement containing regional hazelnut shell ash wastes, Journal of Cleaner Production 259 (2020) 120965.
[31] S. Munshi, R.P. Sharma, Investigation on the pozzolanic properties of rice straw ash prepared at different temperatures, Materials Express 8(2) (2018) 157-164.
[32] N. Kumar, V. Ponnuswami, S. Jeeva, C. Ravindran, D. Kalaivanan, Cashew Industry in India–an overview, Chronica Horticulturae. 52 (2012) 27.
[33] A. Mohod, S. Jain, A. Powar, Cashew nut shell waste: availability in small-scale cashew processing industries and its fuel properties for gasification, International Scholarly Research Notices 2011 (2011).
[34] P. Das, T. Sreelatha, A. Ganesh, Bio oil from pyrolysis of cashew nut shell-characterisation and related properties, Biomass and bioenergy 27(3) (2004) 265-275.
[35] A. Mohod, S. Jain, A. Powar, Cashew nut processing: sources of environmental pollution and standards, BIOINFO Environ Pollut 1(1) (2011) 5-11.
[36] J. James, R. Roshna, S. Santhiya, Cashew nut shell ash as a supplementary additive in lime stabilized expansive soil composites, Materials Today: Proceedings (2022).

[37] S. Oyebisi, T. Igba, D. Oniyide, Performance evaluation of cashew nutshell ash as a binder in concrete production, Case Studies in Construction Materials 11 (2019) e00293.
[38] A. Tantri, G. Nayak, M. Kamath, A. Shenoy, K.K. Shetty, Utilization of cashew nut-shell ash as a cementitious material for the development of reclaimed asphalt pavement incorporated self compacting concrete, Construction and Building Materials 301 (2021) 124197.
[39] S. Oyebisi, T. Igba, A. Raheem, F. Olutoge, Predicting the splitting tensile strength of concrete incorporating anacardium occidentale nut shell ash using reactivity index concepts and mix design proportions, Case Studies in Construction Materials 13 (2020) e00393.
[40] J.K. Mendu, R.M.R. Pannem, Assessment of mechanical properties of cashew nut shell ash blended concrete, Innovative Infrastructure Solutions 6(4) (2021) 1-20.
[41] C. Pavithra, A. Arokiaprakash, A. Maheshwari, Behaviour of concrete adding chicken feather as fibre with partial replacement of cement with Cashewnut shell powder, Materials Today: Proceedings 43 (2021) 1173-1178.
[42] S. Oyebisi, A. Ede, H. Owamah, T. Igba, O. Mark, A. Odetoyan, Optimising the Workability and Strength of Concrete Modified with Anacardium Occidentale Nutshell Ash, Fibers 9(7) (2021) 41.
[43] M.D. Thomas, B. Fournier, K.J. Folliard, Alkali-aggregate reactivity (AAR) facts book, United States. Federal Highway Administration. Office of Pavement Technology, 2013.
[44] I.B.O. MINES, Indian Minerals Yearbook 2016, Gov. India Minist. Mines Nagpur 13 (2018) 1-17.
[45] K.F. Portella, L.E. Lagoeiro, J.L. Bronholo, D.d.C. Miranda, M.D. Bragança, B.G. Dias, N.P. Hasparyk, S.C. Kuperman, Alkali-silica reaction (ASR)-Investigation of crystallographic parameters of natural sands by backscattered electron diffraction, Revista IBRACON de Estruturas e Materiais 14 (2021).
[46] M.A. Noaman, M.N. Islam, M.R. Islam, M.R. Karim, Mechanical properties of brick aggregate concrete containing rice husk ash as a partial replacement of cement, Journal of Materials in Civil Engineering 30(6) (2018) 04018086.
[47] C. ASTM, Standard test method for amount of water required for normal consistency of hydraulic cement paste, (2011).
[48] A. ASTM, Standard test methods for time of setting of hydraulic cement by Vicat needle, ASTM International: West Conshohocken, PA, USA (2013).
[49] B. EN, 196-3: 2016 Methods of testing cement, Determination of setting times and soundness (2016).
[50] C. ASTM, Standard test method for flow of hydraulic cement mortar, C1437 (2007).
[51] A. Standard, ASTM C109-standard test method for compressive strength of hydraulic cement mortars, ASTM International, West Conshohocken, PA (2008).
[52] A. ASTM C642, Standard test method for density, absorption, and voids in hardened concrete, ASTM, ASTM International (2013).
[53] C. Astm, 597, Standard test method for pulse velocity through concrete, ASTM International, West Conshohocken, PA (2009).
[54] P. Ghosh, Q. Tran, Correlation between bulk and surface resistivity of concrete, International Journal of Concrete Structures and Materials 9(1) (2015) 119-132.
[55] L.-H. Yu, H. Ou, L.-L. Lee, Investigation on pozzolanic effect of perlite powder in concrete, Cement and Concrete Research 33(1) (2003) 73-76.
[56] K. Umamaheswaran, V.S. Batra, Physico-chemical characterisation of Indian biomass ashes, Fuel 87(6) (2008) 628-638.

[57] Y. Niu, H. Tan, Ash-related issues during biomass combustion: Alkali-induced slagging, silicate melt-induced slagging (ash fusion), agglomeration, corrosion, ash utilization, and related countermeasures, Progress in Energy and Combustion Science 52 (2016) 1-61.
[58] T. Akinhanmi, V. Atasie, P. Akintokun, Chemical composition and physicochemical properties of cashew nut (Anacardium occidentale) oil and cashew nut shell liquid, Journal of Agricultural, Food and Environmental Sciences 2(1) (2008) 1-10.
[59] E. Gyedu-Akoto, Utilization of some cashew by-products, Nutrition & Food Science (2011).
[60] R. Rico, M. Bulló, J. Salas-Salvadó, Nutritional composition of raw fresh cashew (Anacardium occidentale L.) kernels from different origin, Food science & nutrition 4(2) (2016) 329-338.
[61] A. Aweto, M. Ishola, The impact of cashew (Anacardium occidentale) on forest soil, Experimental Agriculture 30(3) (1994) 337-341.
[62] Z. Li, K. Afshinnia, P.R. Rangaraju, Effect of alkali content of cement on properties of high performance cementitious mortar, Construction and Building Materials 102 (2016) 631-639.
[63] S. Damerio, P. Nukala, J. Juraszek, P. Reith, H. Hilgenkamp, B. Noheda, Structure and magnetic properties of epitaxial CaFe2O4 thin films, npj Quantum Materials 5(1) (2020) 1-10.
[64] A. Bloesser, J. Timm, H. Kurz, W. Milius, S. Hayama, J. Breu, B. Weber, R. Marschall, A novel synthesis yielding macroporous CaFe2O4 sponges for solar energy conversion, Solar RRL 4(8) (2020) 1900570.
[65] N.M. Al-Akhras, M. Abdulwahid, Utilisation of olive waste ash in mortar mixes, Structural Concrete 11(4) (2010) 221-228.
[66] D. Adesanya, A. Raheem, Development of corn cob ash blended cement, Construction and Building Materials 23(1) (2009) 347-352.
[67] K.M.A. Hossain, Blended cement using volcanic ash and pumice, Cement and Concrete research 33(10) (2003) 1601-1605.
[68] M. Thomas, Supplementary cementing materials in concrete, CRC press2013.
[69] M. Tokyay, Cement and concrete mineral admixtures, CRC Press2016.
[70] M. Liu, H. Tan, X. He, Effects of nano-SiO2 on early strength and microstructure of steam-cured high volume fly ash cement system, Construction and Building Materials 194 (2019) 350-359.
[71] J. Chen, S.-c. Kou, C.-s. Poon, Hydration and properties of nano-TiO2 blended cement composites, Cement and Concrete Composites 34(5) (2012) 642-649.
[72] L. Wang, Q. Li, J. Song, S. Liu, Effect of graphene oxide on early hydration and compressive strength of Portland cement-copper tailing powder composite binder, Powder Technology 386 (2021) 428-436.
[73] I. EN, 197-1: Cement—Composition, Specifications and Conformity Criteria for Common Cements. No. BS EN 197-1: 2011, British Standards Institution (BSI): London, UK (2011).
[74] C. Bhojaraju, S.S. Mousavi, V. Brial, M. DiMare, C.M. Ouellet-Plamondon, Fresh and hardened properties of GGBS-contained cementitious composites using graphene and graphene oxide, Construction and Building Materials 300 (2021) 123902.
[75] Z. Pan, L. He, L. Qiu, A.H. Korayem, G. Li, J.W. Zhu, F. Collins, D. Li, W.H. Duan, M.C. Wang, Mechanical properties and microstructure of a graphene oxide–cement composite, Cement and Concrete Composites 58 (2015) 140-147.
[76] S. Mantellato, M. Palacios, R.J. Flatt, Relating early hydration, specific surface and flow loss of cement pastes, Materials and Structures 52(1) (2019) 1-17.

[77] Y. Bu, J. Weiss, The influence of alkali content on the electrical resistivity and transport properties of cementitious materials, Cement and Concrete Composites 51 (2014) 49-58.
[78] F.F. Ataie, K.A. Riding, Thermochemical pretreatments for agricultural residue ash production for concrete, Journal of Materials in Civil Engineering 25(11) (2013) 1703-1711.
[79] S. Praveenkumar, G. Sankarasubramanian, S. Sindhu, Strength, permeability and microstructure characterization of pulverized bagasse ash in cement mortars, Construction and Building Materials 238 (2020) 117691.
[80] R. Rajamma, R.J. Ball, L.A. Tarelho, G.C. Allen, J.A. Labrincha, V.M. Ferreira, Characterisation and use of biomass fly ash in cement-based materials, Journal of hazardous materials 172(2-3) (2009) 1049-1060.
[81] Q. Li, Y. Zhao, H. Chen, P. Zhao, P. Hou, X. Cheng, N. Xie, Effect of waste corn stalk ash on the early-age strength development of fly ash/cement composite, Construction and Building Materials 303 (2021) 124463.
[82] L. Huang, P. Yan, Effect of alkali content in cement on its hydration kinetics and mechanical properties, Construction and Building Materials 228 (2019) 116833.
[83] B. Alabadan, M. Olutoye, M. Abolarin, M. Zakariya, Partial replacement of ordinary Portland cement (OPC) with bambara groundnut shell ash (BGSA) in concrete, Leonardo Electronic Journal of Practices and Technologies 6 (2005) 43-48.
[84] C. ASTM, 270. Standard Specification for Mortar for Unit Masonry, Especificación Estándar del Mortero para Unidades de Mampostería (2003).
[85] A. C90, Standard Specification for Loadbearing Concrete Masonry Units, Annual book of ASTM standards, United States (2014).
[86] M. Shakouri, C.L. Exstrom, S. Ramanathan, P. Suraneni, J.S. Vaux, Pretreatment of corn stover ash to improve its effectiveness as a supplementary cementitious material in concrete, Cement and Concrete Composites 112 (2020) 103658.
[87] V.M. Malhotra, Testing hardened concrete: nondestructive methods, (1976).
[88] E. Mohseni, F. Naseri, R. Amjadi, M.M. Khotbehsara, M.M. Ranjbar, Microstructure and durability properties of cement mortars containing nano-TiO2 and rice husk ash, Constr. Build. Mater 114 (2016) 656-664.
[89] F. Saint-Pierre, A. Philibert, B. Giroux, P. Rivard, Concrete quality designation based on ultrasonic pulse velocity, Construction and Building Materials 125 (2016) 1022-1027.
[90] J.R. Leslie, W. Cheesman, An ultrasonic method of studying deterioration and cracking in concrete structures, Journal of the American Concrete Institute 21(1) (1949) 17-36.
[91] N.R.C.o.C.D.o.B. Research, R. Feldman, Non-destructive testing of concrete, 1977.
[92] C. Costa, J.C. Marques, Feasibility of eco-friendly binary and ternary blended binders made of fly-ash and oil-refinery spent catalyst in ready-mixed concrete production, Sustainability 10(9) (2018) 3136.
[93] H. Xiong, K. Yuan, J. Xu, M. Wen, Pore structure, adsorption, and water absorption of expanded perlite mortar in external thermal insulation composite system during aging, Cement and Concrete Composites 116 (2021) 103900.
[94] B.S. Thomas, J. Yang, K.H. Mo, J.A. Abdalla, R.A. Hawileh, E. Ariyachandra, Biomass ashes from agricultural wastes as supplementary cementitious materials or aggregate replacement in cement/geopolymer concrete: A comprehensive review, Journal of Building Engineering 40 (2021) 102332.
[95] K. Selvaranjan, J. Gamage, G. De Silva, S. Navaratnam, Development of sustainable mortar using waste rice husk ash from rice mill plant: Physical and thermal properties, Journal of Building Engineering 43 (2021) 102614.

[96] A. Nanni, Guide for the design and construction of concrete reinforced with FRP bars (ACI 440.1 R-03), Structures Congress 2005: Metropolis and Beyond, 2005, pp. 1-6.
[97] T. Bremner, K. Hover, R. Poston, J. Broomfield, T. Joseph, R. Price, K. Clear, M. Khan, D. Reddy, J. Clifton, Protection of metals in concrete against corrosion, Technical Report for ACI Committee 222: Farmington Hills, MI, USA2001.
[98] J. Gonzalez, J. Miranda, S. Feliu, Considerations on reproducibility of potential and corrosion rate measurements in reinforced concrete, Corrosion Science 46(10) (2004) 2467-2485.
[99] C. Bhojaraju, S.S. Mousavi, C.M. Ouellet-Plamondon, Influence of GGBFS on corrosion resistance of cementitious composites containing graphene and graphene oxide, Cement and Concrete Composites 135 (2023) 104836.
[100] K.G. Babu, P.S. Prakash, Efficiency of silica fume in concrete, Cement and concrete research 25(6) (1995) 1273-1283.
[101] K.G. Babu, G.S.N. Rao, Efficiency of fly ash in concrete, Cement and Concrete Composites 15(4) (1993) 223-229.
[102] L.K. Turner, F.G. Collins, Carbon dioxide equivalent (CO2-e) emissions: A comparison between geopolymer and OPC cement concrete, Construction and building materials 43 (2013) 125-130.
[103] R.H. Crawford, A. Stephan, F. Prideaux, Environmental Performance in Construction (EPiC) Database, 2019.
[104] M.F. Alnahhal, U.J. Alengaram, M.Z. Jumaat, F. Abutaha, M.A. Alqedra, R.R. Nayaka, Assessment on engineering properties and CO2 emissions of recycled aggregate concrete incorporating waste products as supplements to Portland cement, Journal of cleaner production 203 (2018) 822-835.
[105] CEA, CO2 Baseline Database for the Indian Power Sector, User Guide, 2018.
[106] C. Gajjar, A. Sheikh, India specific road transport emission factors, Transport Sector Emission Factor Methodologies (2015) 9-10.
[107] F. Collins, Inclusion of carbonation during the life cycle of built and recycled concrete: influence on their carbon footprint, The International Journal of Life Cycle Assessment 15(6) (2010) 549-556.
[108] D. Dissanayake, C. Jayasinghe, M. Jayasinghe, A comparative embodied energy analysis of a house with recycled expanded polystyrene (EPS) based foam concrete wall panels, Energy and Buildings 135 (2017) 85-94.
[109] M. Ibrahim, A. El Berry, K. Ashour, EXPERIMENTAL AND THEORETICAL STUDY OF SMART ENERGY MANAGEMENT SOLAR WATER HEATING SYSTEM FOR OUTDOOR SWIMMING POOL APPLICATION IN EGYPT, Frontiers in Heat and Mass Transfer (FHMT) 18 (2022).
[110] N. Bheel, S.K. Mahro, A. Adesina, Influence of coconut shell ash on workability, mechanical properties, and embodied carbon of concrete, Environmental science and pollution research 28(5) (2021) 5682-5692.
[111] G. Srikanth, A. Fernando, K. Selvaranjan, J. Gamage, L. Ekanayake, Development of a plastering mortar using waste bagasse and rice husk ashes with sound mechanical and thermal properties, Case Studies in Construction Materials 16 (2022) e00956.
[112] R. Kumar, N. Shafiq, A. Kumar, A.A. Jhatial, Investigating embodied carbon, mechanical properties, and durability of high-performance concrete using ternary and quaternary blends of metakaolin, nano-silica, and fly ash, Environmental Science and Pollution Research 28(35) (2021) 49074-49088.